

1 **Lost islands in the northern Lesser Antilles: possible milestones in the Cenozoic**
2 **dispersal of terrestrial organisms between South-America and the Greater Antilles**
3

4

5 **Jean-Jacques Cornée¹, Philippe Münch², Mélody Philippon¹, Marcelle BouDagher-**
6 **Fadel³, Frédéric Quillévéré⁴, Mihaela Melinte-Dobrinescu⁵, Jean-Frédéric Lebrun¹,**
7 **Aurélien Gay², Solène Meyer^{2, 6}, Lény Montheil², Serge Lallemand², Boris Marcaillou⁶,**
8 **Muriel Laurencin⁷, Lucie Legendre¹, Clément Garrocq², Milton Boucard¹, Marie-Odile**
9 **Beslier⁶, Mireille Laigle⁶, Laure Schenini⁶, Pierre-Henri Fabre⁸, Pierre-Olivier Antoine⁸,**
10 **Laurent Marivaux⁸ and the GARANTI and ANTITHESIS Scientific Parties.**

11

12 *The GARANTI Scientific Party is composed of:*

13 Agranier, A., Arcay, D., Audemard, F., Beslier, M.O., Boucard, M; Cornée, J.J., Fabre, M.,
14 Gay, A., Graindorge, D., Klingelhofer, A. Heuret, F., Laigle, M., Lallemand, S., Lebrun J.F.,
15 Léticée, J.L., Malengro, D., Marcaillou, B., Mercier de Lepinay, B., Münch, P., Olliot, E.,
16 Oregioni, D., Padron, C., Quillévéré, F., Ratzov, G., Schenini, L. and Yates, B., J.F.

17

18 *The ANTITHESIS Scientific Party is composed of:* Bouquerel, H., Conin, M., Crozon, J., Dellong,
19 D., De Min, L., de Voogd, B., Evain, M., Fabre, M., Graindorge, D., Gwandai, W., Heuret,
20 A., Klingelhofer, F., Laigle, M., Lallemand, S., Laurencin, M., Lebrun, J.-F., Legendre, L.,
21 Lucazeau, F., Mahamat, H., Marcaillou, B., Mazabraud, Y., Pichot, T., Prunier, C., Renouard,
22 A., Rolandonne, F., Rousset, D., Schenini, L., Thomas, Y., Vitard C.

23

24 ¹ *Géosciences Montpellier, CNRS-Université des Antilles-Université de Montpellier, F-97159*

25 *Pointe à Pitre, Guadeloupe, France*

26 ² *Géosciences Montpellier, CNRS-Université de Montpellier-Université des Antilles, F-34095*

27 *Montpellier, France*

28 ³ *Office of the Vice-Provost (Research), University College London, 2 Taviton Street, London*

29 *WC1H 0BT, UK*

30 ⁴ *Université Claude Bernard Lyon 1, ENS de Lyon, CNRS, UMR 5276 LGL-TPE, F-69622*

31 *Villeurbanne, France*

32 ⁵ *National Institute of Marine Geology and Geoecology, 23–25 Dimitrie Onciul Street, PO*
33 *Box 34–51, 70318 Bucharest, Romania*

34 ⁶ *Geoazur, Université de la Côte d'Azur, CNRS, Observatoire de la Côte d'Azur, IRD, F-*
35 *06560 Valbonne, France*

36 ⁷ *Laboratoire d'Océanologie et Géosciences, Université de Lille, 59655 Villeneuve d'Ascq,*
37 *France*

38 ⁸ *Institut des Sciences de l'Evolution de Montpellier (ISE-M), Univ Montpellier, CNRS, IRD,*
39 *EPHE, F-34095 Montpellier, France*

40
41 Corresponding author: Jean-Jacques Cornée, jean-jacques.cornee@gm.univ-montp2.fr

42 Université des Antilles, Dépt. Géologie, Campus de Fouillole, F-97159 Pointe à Pitre Cedex,
43 Guadeloupe, FWI

44

45 **Keywords: Lesser Antilles, Cenozoic basins, biostratigraphy, seismic stratigraphy,**
46 **palaeogeography, vertical motions**

47

48 **ABSTRACT**

49 Our study aims to reconstruct the palaeogeography of the northern part of the Lesser Antilles in order
50 to analyse whether emerged areas might have existed during the Cenozoic, favouring terrestrial faunal
51 dispersals between South America and the Greater Antilles along the present-day Lesser Antilles arc.
52 The stratigraphy and depositional environments of the islands of Anguilla, St Martin, Tintamarre, St
53 Barthélemy, Barbuda and Antigua are reviewed in association with multichannel reflection seismic
54 data acquired offshore since the 80's in the Saba, Anguilla and Antigua Banks and in the Kalinago Basin,
55 including the most recent academic and industrial surveys. Seven seismic megasequences and seven
56 regional unconformities are defined, and calibrated from deep wells on the Saba Bank and various
57 dredges performed during marine cruises since the 70's in the vicinity of the islands. Onshore and
58 offshore correlations allow us to depict an updated and detailed sedimentary organisation of the
59 northern part of the Lesser Antilles from the late Eocene to the late Pleistocene. Paleogeographic
60 reconstructions reveal sequences of uplift and emergence across hundredswide areas during the late
61 Eocene, the late Oligocene, the early middle-Miocene and the latest Miocene-earliest Pliocene,
62 interspersed by drowning episodes. The ~200 km-long and ~20 km-wide Kalinago Basin opened as an
63 intra-arc basin during the late Eocene - early Oligocene. These periods of emergence may have
64 favoured the existence of episodic mega-islands and transient terrestrial connections between the

65 Greater Antilles, the Lesser Antilles and the northern part of the Aves Ridge (Saba Bank). During the
66 Pleistocene, archipelagos and mega-islands formed repeatedly during glacial maximum episodes.

67

68 **1. INTRODUCTION**

69

70 The Caribbean, including the Greater and Lesser Antilles located at the northeastern edge
71 of the Caribbean Plate, are regarded as one of the most important centres of insular biodiversity
72 (Myers al., 2000; Mittermeier et al., 2011). Despite decades of studies, the phylogenetic origins
73 and historical biogeography of this astonishing biodiversity remain, however, controversial
74 (e.g., Hedges et al., 1992; MacPhee and Iturralde-Vinent, 1995, 2005; Iturralde-Vinent and
75 MacPhee, 1999; Myers et al., 2000; Hedges, 2001, 2006; Ali, 2012). In an island setting, either
76 over-water transports (natural rafts of matted vegetation) or land connections provide possible
77 routes for dispersal of terrestrial organisms and their colonization of these remote Caribbean
78 islands. If over-water dispersals by rafting are sweepstake dispersals (and as such hardly
79 predictable), the possibility of over-land (via land-bridges) dispersals relies on the regional
80 tectono-magmatic evolution of the Lesser Antilles subduction zone.

81 Biogeographic models for Antillean terrestrial organisms derive from limited
82 palaeontological and phylogenetic inferences (either based on the morphology or on
83 genes/proteins of living and recently extinct species) (Hedges, 1996; Woods et al., 2001;
84 Graham, 2003; Roca et al., 2004; MacPhee, 2005; Fabre et al., 2014; Brace et al., 2015, 2016;
85 Courcelle et al., 2019; Delsuc et al., 2019; Presslee et al., 2019; Marivaux et al., 2020). They
86 also derive from still controversial paleogeographic models of the Caribbean Plate evolution
87 (e.g., Stephan et al., 1990; Iturralde-Vinent and MacPhee, 1999; Pindell and Kennan, 2009) and
88 global reconstructions (Blakey, <https://deeptimemaps.com/>; Scotese; 2016). The main
89 discussed model for explaining the arrival of many terrestrial organisms of South American
90 origin on the Caribbean islands relate to a possible 2 Myrs- long period of subaerial exposure

91 of the Aves Ridge (Fig. 1) at the Eocene-Oligocene transition. Following this model, the ridge
92 momentarily constituted a land-bridge (named GAARlandia, for land of **G**reater **A**ntilles–**A**ves
93 **R**idge) between northern South America and the Greater Antilles (e.g., MacPhee and Iturralde-
94 Vinent, 1995; Iturralde-Vinent and MacPhee, 1999; MacPhee, 2005; Iturralde-Vinent, 2006)).

95 Contrary to the Aves Ridge, the potential contribution of the Lesser Antilles in early
96 dispersals of South American faunas and flora has never been considered. This is paradoxical
97 because the archipelago is located closer to the subduction deformation front and has
98 experienced uplift and drowning events likely favouring land-organism dispersals and
99 subsequent insular evolution. This is particularly obvious in the Guadeloupe archipelago where
100 repeated uplifts, leading to subaerial exposures, and subsequent drownings have been evidenced
101 (Cornée et al., 2012; Münch et al., 2013, 2014; De Min et al., 2014). Further north, it has been
102 proposed that the Pleistocene rodent *Amblyrhiza*, an endemic giant chinchilloid caviomorph
103 from Anguilla, St Martin and St Barthélemy islands, could be closely related to early Oligocene
104 chinchilloids from Puerto Rico (Velez-Juarbe et al., 2014; Marivaux et al., 2020), thereby
105 extending the evolutionary history of this rodent group back to 30 Ma, and revealing its
106 widespread distribution between the Greater Antilles and the northern Lesser Antilles through
107 time.

108 In this work, we study the palaeogeographic evolution of the northeastern part of the Lesser
109 Antilles during the Cenozoic, as it may have constituted an episodic emerged area between the
110 Aves Ridge to the southwest and the Greater Antilles to the North: the GrANoLA land -Greater
111 Antilles- Northern Lesser Antilles land (Philippon et al., 2020a). Previous bathymetric
112 reconstructions and offshore-onshore geological investigations have suggested that the
113 Kalinago intra-arc rift basin (Figs. 1, 2) may have undergone substantial vertical motion (e.g.,
114 Bouysse et al., 1985a; Mann et al., 1995; Feuillet et al., 2011) and 15% extension (Legendre et
115 al., 2018). In the whole Eastern Caribbean (Aves Ridge, Greater and Lesser Antilles), accurate

116 constraints on the chronology, duration and spatial extent of land emergence and drowning
117 during the Cenozoic are, however, strongly missing to reconstruct the regional paleogeographic
118 evolution. This lack of information prevents the effective testing of biogeographic models
119 deriving from gene-based and morpho-anatomical phylogenies and associated divergence time
120 estimates. In this work, we refine the sedimentology and stratigraphy of the deposits over an
121 area extending from the Saba Bank to the Antigua Bank encompassing the Kalinago Basin
122 (Figs. 1, 2), and use these analyses to reconstruct the vertical motions that occurred in this key
123 area of the Northern Lesser Antilles. The study is based on new onshore palaeoenvironmental,
124 biostratigraphic, and structural data, combined and correlated with new offshore-dredged
125 samples and seismostratigraphic interpretation of seismic reflection data from the
126 ANTITHESIS (Marcaillou and Klingelhoefer, 2013; 2016) and GARANTI cruises (Lebrun and
127 Lallemand, 2017), which allow us to reconstruct the palaeogeographic evolution of the region.

128

129 **2. TECTONO-MAGMATIC EVOLUTION OF THE NE CARIBBEAN SINCE THE** 130 **CRETACEOUS**

131

132 The westward subduction of the Proto-Caribbean/Atlantic Ocean lithosphere beneath the
133 Caribbean Plate initiated from Cuba southward during the Cretaceous. The Great Arc of the
134 Caribbean (GAC) is the magmatic expression of this subduction. Magmatic arc samples from
135 the southern Aves Ridge and Leeward Antilles offshore Venezuela indicate that subduction
136 occurred there since the middle-late Cretaceous (Coniacian; Neill et al., 2011) or after
137 Santonian (Hastie et al., 2021). During the Paleocene and the early Eocene, the motion of the
138 North American Plate relative to the Caribbean plate changed from north-eastward to eastward
139 (Pindell and Kennan, 2009; Boschman et al., 2014). At the same time, the collision of the
140 Bahamas Bank margin with the Caribbean Plate sutured the subduction along its northern part

141 (accreting Cuba to the North American plate) whereas a new E-W trending transform plate
142 boundary formed along the proto-Cayman Trough that started opening (e.g., Pindell and
143 Kennan, 2009; Boschman et al., 2014). Subsequently, the Greater Antilles underwent sinistral
144 shearing and were dismembered along the new transform plate boundary (Fig. 1). The present-
145 day trench curvature of the northern Lesser Antilles subduction zone and along strike variation
146 of the convergence obliquity most likely results from this Eocene reorganisation of the plate
147 boundary and subsequent left lateral motion of the Bahamas Bank / Cuba margin relative to the
148 Caribbean Plate interior (Boschman et al., 2014; Philippon and Corti, 2016; Philippon et al.,
149 2020b). Today, the Greater and Lesser Antilles margins are separated by an elongated, fault-
150 bounded basin, the Anegada Trough (e.g., Jany et al., 1990; Laurencin et al., 2017 and
151 references therein; Fig. 1). Based on dredged samples and seismic reflection profiles, the
152 opening of the Anegada Trough is supposed to have occurred during the middle or the late
153 Miocene (Jany et al., 1990), and its activity has probably been negligible since 2 Ma (Chaytor
154 and ten Brink, 2015; Calais et al., 2016). Our study area lies south of this major tectonic
155 structure separating the Greater from the Lesser Antilles (Fig. 1).

156 Three phases of arc magmatism are recognized along the Antillean subduction zone, with
157 lateral variation with time:

158 (i) arc magmatism was first established during the Late Cretaceous-Paleocene along the
159 Aves Ridge (Fig. 1) as part of the GAC (ages of arc magmatic rocks range between 88 Ma and
160 59 Ma; Fox et al., 1971; Bouysse et al., 1985a; Neill et al., 2011).

161 (ii) The GAC then migrated eastward (*i.e.*, trenchward) probably during the middle Eocene,
162 as evidenced by the occurrence of Lutetian lavas in the Grenadines Islands (Westercamp et al.,
163 1985). This Eocene arc is present beneath the southern Lesser Antilles islands, and, from
164 Martinique northward, Eocene to earliest Miocene remnants of this arc are exposed and dated
165 in the forearc domain (Westercamp, 1988; Bouysse and Westercamp, 1990; Legendre et al.,

166 2018) (Fig. 1). Along the northern Lesser Antilles, this arc is exposed and dated based on
167 radiometric data in Antigua (middle Eocene to earliest Miocene; Nagle et al., 1976; Briden et
168 al., 1979; Mascle and Westercamp, 1983; Weiss, 1994), St Barthélemy (middle Eocene to latest
169 Oligocene; Legendre et al., 2018), and St Martin (late Eocene to early Oligocene; Nagle et al.,
170 1976; Briden et al., 1979). Late Paleogene volcanoclastic arc (or backarc) rocks have also been
171 found in deformed zones of the Virgins Islands, Puerto-Rico and Anguilla (Briden et al., 1979;
172 Andréieff et al., 1988; Jolly et al., 1998; Rankin, 2002), thereby suggesting that the remnant arc
173 extended across the incipient Anegada Trough at this time. These rocks, nevertheless, have
174 never been related neither to those of the Aves Ridge nor to those of the Grenada Basin.

175 (iii) The modern arc (inner arc of Mc Cann and Sykes, 1984) is formed 50 km west of the late
176 Paleogene-early Neogene remnant one (outer arc of Mc Cann and Sykes, 1984). From
177 Guadeloupe northward, volcanism occurred since the early Pliocene (e.g., Samper et al., 2007;
178 Favier et al., 2019; Carey et al., 2020). The northernmost island of the arc is Saba where
179 volcanism occurred during the Late Pleistocene (Defant et al., 2001). Offshore north of Saba,
180 Pliocene volcanic and volcanoclastic rocks have been dredged from the Luymes Bank (cruise
181 ARCANTE 1) and the Noroît Seamount (cruise ARCANTE 3, 118) (Figs. 1 and 2) (Bouysse et
182 al., 1981; 1985b).

183

184 **3. GEOLOGICAL SETTING OF THE NE CARIBBEAN ISLANDS**

185

186 **3.1. Anguilla Bank**

187 Three main islands emerge from the large, shallow water Anguilla Bank: from north to
188 south Anguilla, St Martin (including the islet of Tintamarre) and St Barthélemy (Fig. 2).
189 Neogene deposits are exposed on these three islands (Christman 1953; Andréieff et al., 1987;
190 1988; older references therein).

191 St Martin consists of 2000 to 3000 m-thick Eocene volcanoclastic turbidites intruded by
192 late Eocene-early Oligocene granodiorites (28.4-31.3 Ma; Nagle et al., 1976; Briden et al.,
193 1979). In the southwestern part of the island, late Oligocene magmatic rocks may also occur
194 but remain undated (Andréieff et al., 1988, 1989). On the southwestern and eastern margins of
195 the island, Neogene carbonates deposited unconformably on Paleogene rocks, which were tilted
196 along a NE-SW fault bounding the northwestern coast of the island. Drilled cores from the
197 southwestern deposits recovered up-to-250 m of Neogene carbonates along the margin of the
198 island (Terres Basses; Dagain et al., 1989). On the islet of Tintamarre, the basal part of the
199 Neogene deposits remains unknown. According to Andréieff et al. (1988), the deposits at St
200 Martin and Tintamarre constitute two main formations with unknown relationships: 1) > 70 m-
201 thick sedimentary rocks which were deposited during the late Burdigalian in a reefal
202 depositional setting; 2) 80 m- thick distal forereef sedimentary rocks which were deposited
203 between the late Serravallian and the Messinian in St Martin only.

204 In the island of Anguilla, the oldest sedimentary deposits consist of late Paleocene to
205 Eocene volcanoclastic turbidites tilted to the south-east (Andréieff et al., 1988). These turbidites
206 are unconformably overlaid by a 100 m- thick biostromal coral reef deposit considered to be
207 either early Miocene or middle Miocene (Andréieff et al., 1988; Budd et al., 2005). Shallow
208 water carbonates are poorly known from other islets of the Anguilla Bank, Sombrero (Pliocene)
209 and Dog Islands (late Burdigalian-early Langhian; Bouysse et al., 1985a; Andréieff et al., 1987).

210 During the cruises ARCANTE, dredged samples have been collected on flanks of the
211 Anguilla Bank (Bouysse and Guennoc, 1983; Bouysse et al., 1985a) (Fig. 2). On the
212 southwestern margin of the Anguilla Bank, dredges 46V and 47V yielded Pleistocene to
213 Holocene carbonate sediments. On the northern margin, dredge 121D provided Pliocene-?
214 Pleistocene tuff limestones, Serravallian marls, and late Eocene magmatic rocks (36.5 to 33 Ma
215 interval, whole rock K-Ar ages; Bouysse et al., 1985a). Finally, to the east of the Bank, dredges

216 E402 and ST31 yielded uppermost Cretaceous radiolarian-bearing limestones and Pleistocene
217 clays, respectively.

218

219 **3.2. *Kalinago Basin***

220 The Kalinago Basin is a NW-SE trending, 100 km- long intra-arc rift separating the
221 Anguilla Bank from the recent active volcanic arc (Bouysse et al., 1985a; Jany et al., 1990)
222 (Fig. 2). The basin is bounded by syn- to post- Neogene faults and possibly comprise deformed,
223 Cretaceous to Oligocene or Miocene rocks overlain by poorly deformed, 2.000 m- thick
224 Neogene to Pleistocene deposits (Jany, 1989; Jany et al., 1990; Church and Allison, 2004). At
225 the northern margin of the basin on slopes of the Aguillita Spur, dredge RV-Eastward 1390
226 (Fig. 2) yielded clays and marls that were deposited between the Pliocene and the Pleistocene
227 (Jany, 1989). In the southern part of the basin, southeast of Montserrat (Fig. 2), the Integrated
228 Ocean Drilling Program (IODP) Leg 340 (out of Fig. 2) drilled 181 m of late Pleistocene
229 volcanoclastic deposits (Coussens et al., 2012).

230

231 **3.3. *Saba Bank***

232 The shallow water Saba Bank (Figs. 1 and 2) has been intensively explored for oil
233 prospecting (Warner, 1990; Larue and Warner, 1991; Daly, 1995; Church and Allison, 2004;
234 Matchette-Downes, 2007). On the basis of seismic investigations and wells SBD1 (total depth
235 of 2977 m; Marathon Group) and SBD2 (total depth of 4231 m; Fina Group), the bank
236 comprises from bottom to top: 1) a deformed Cretaceous to Paleocene sedimentary basement
237 topped by an unconformity; 2) a subaerial, at least 120 m- thick, porphyritic andesitic sequence
238 dated at 34.4 ± 3.7 Ma and 37.3 ± 1.4 Ma (whole rock K-Ar); 3) a *ca* 900 to 1000 m- thick
239 “turbidite” unit dated from the early late Eocene to the early Oligocene based on planktonic
240 foraminifera and calcareous nannofossils; this unit correlates with late Eocene reefs developed

241 on palaeostructural highs; 4) a *ca* 1500 m- thick volcanoclastic “fluvio-deltaic” unit, which were
242 deposited between the early late Oligocene and the early Miocene based on calcareous
243 nannofossils and benthic foraminifera, and 5) an “upper carbonate unit”, which was deposited
244 between the middle Miocene and the early Pliocene based on planktonic foraminifera, and
245 which indicates a shallowing-upward trend (Church and Allison, 2004).

246 North of the Saba Bank, a Pliocene (*ca* 4 Ma) volcanic activity has been evidenced on
247 the Luymes Bank and the Noroît Seamount and may correspond to the northeastern termination
248 of the active volcanic Lesser Antilles Arc (Bouysse et al., 1985a; b). Along with volcanic rocks
249 and clasts, Pliocene-Pleistocene pelagic limestones were mainly recovered and coral reefs and
250 red-algal limestones were also dredged. Finally, one dredge (119D) south of the Noroît
251 Seamount yielded some porphyritic andesite fragments dated at 66.5 ± 1.5 Ma (whole rock K-
252 Ar; Bouysse et al., 1985a), corresponding, like in the Saba Bank and St Croix Island, to the
253 Maastrichtian-Danian GAC basement (Speed et al., 1979) (Fig. 2).

254

255 **3.4. Antigua Bank**

256 The Antigua island comprises three main lithostratigraphic units with an estimated total
257 thickness of 2.500 m. These units are tilted northeastward on the footwall of the normal faults
258 forming the NE side of the Kalinago Basin (e.g., Martin Kayes, 1969; Frost and Weiss, 1979;
259 Mascle and Westercamp, 1983; Multer et al., 1986; Weiss, 1994; Donovan et al., 2014;
260 Robinson et al., 2017): 1) the Basal Volcanic Complex (1500 m- thick), poorly constrained as
261 either middle Eocene or Oligocene (39.7-23 Ma; *in* Briden et al., 1979); 2) the Central Plain
262 Group (500 m- thick), composed of volcanoclastic deposits with freshwater and marine
263 limestones, supposed to have been deposited during the Oligocene (Mascle and Westercamp,
264 1983; Robinson et al., 2017); 3) the late Oligocene Antigua Formation, composed of shallow
265 water limestones evolving eastward into deep marine limestones.

266 The Barbuda island consists of four shallow water carbonate formations (Fm.) separated
267 by subaerial erosional surfaces (Brasier and Mather, 1975), from bottom to top: the Highland
268 Fm. (bank edge facies, 40 m- thick at least), Beazer Fm. (fringing reefs, 5 m- thick; Pleistocene),
269 Codrington Fm. (fringing and barrier reefs, 5 m- thick; late Pleistocene) and Palmetto Fm.
270 (eolian dunes, reef, lagoon, and beach deposits, 10 m- thick; Holocene). The age of the Highland
271 Fm. is still debated: Oligocene (Reed, 1921), middle Miocene (Brasier and Mather, 1975), early
272 Pliocene (Brasier and Donahue, 1985; Watters et al., 1991) or Pleistocene (Russell and Mc
273 Intire, 1966; Land et al., 1967; Martin Kaye, 1969).

274 Four dredges performed during the ARCANTE cruises provided reliable information
275 (Andréieff et al, 1980; Bouysse and Guennoc, 1983) (Fig. 2). On the western margin of the
276 Antigua Bank (also eastern margin of the Kalinago rift), dredge 71D yielded Pliocene to
277 Pleistocene bioclastic limestones from an outer reef depositional setting. On the eastern side of
278 the bank, dredge 79D, collected between 1,800 and 2,000 m depths, yielded late Oligocene
279 carbonates from outer-ramp setting and early Miocene pelagic micritic limestones. Above, at
280 480 m depth, dredge 80D yielded late Miocene marls and Pliocene pelagic carbonate deposits.
281 On top the of the bank, at 30 m depth, dredge 78V yielded recent reefal limestones.

282

283 **4. METHODS AND DATA**

284

285 ***4.1. Rock-samples analyses***

286 New field investigations were conducted in 2015, 2017 and 2020 onshore in Anguilla,
287 St Martin and Tintamarre islands with respectively 7, 7 and 6 logged and sampled sections
288 (Appendices C, D, E). For biostratigraphic analyses, 18 samples were collected in Anguilla, 17
289 in St Martin and 24 in Tintamarre. Combined with field-investigations and sedimentological
290 information, the biostratigraphic analyses allow a correlation between the sections and provide

291 a revised lithostratigraphic sketch of the onshore Neogene deposits of the Anguilla Bank. This
292 onshore sampling was completed by seven offshore carbonate samples collected from three
293 rock-dredge hauls carried out during the GARANTI cruise (Fig. 2): Dredge DR GA-04-01 was
294 collected on the northern steepest flank of the Martinita Seamount; Dredge DR GA-04-02 was
295 collected on the southern flank of this Martinita Seamount
296 ; and Dredge GA-03-01 was collected on the Southeastern Spur (Appendix I). For the island of
297 St Barthélemy, we use the recently published results of Cornée et al. (2020) (Appendix G). In
298 Barbuda, we logged and sampled the Highland Fm. (Appendix F) in 2006; 19 samples were
299 collected. In Antigua, 10 samples were chosen for thin sections in order to refine the age of the
300 Antigua Fm. (Appendix G).

301 Across the whole studied area, a total of 125 polished thin sections were obtained from
302 each carbonate rock-type sample in order to analyse their microfacies and fossil content. The
303 identified microfacies were attributed to a depositional environment following the classification
304 of Wright and Burchette (1996), supplemented by the larger benthic foraminiferal content
305 (BouDagher-Fadel, 2008) (e.g., Appendix B). In addition, 18 soft rock samples were washed
306 over a 65 μm screen and the residues were analysed for foraminiferal biostratigraphy. Finally,
307 standard smear-slides were also prepared for 14 of these soft rock samples for calcareous
308 nannofossil analyses (Appendix A). Our biostratigraphical analyses are based on a complete
309 inventory of larger benthic foraminifera, planktonic foraminifera and calcareous nannofossil
310 taxa found in the thin sections and standard smear-slides. We used the zonal schemes and bio-
311 events calibrations of BouDagher-Fadel (2013, 2015, 2018) for planktonic and larger benthic
312 foraminifera, and those of Backman et al. (2012) for calcareous nannofossils, which have been
313 calibrated against the time scale of Gradstein et al. (2012).

314 Finally, we used the $\text{Ar}^{40}/\text{Ar}^{39}$ method to date a large boulder (50 cm) of a fresh porphyritic
315 andesite reworked in submarine lahar deposits overlain by Neogene limestones in the
316 southwestern part of St Martin Island (details are given in Appendix K).

317

318 *4.2. Seismic reflection profiles*

319 We analyzed eight new profiles from the GARANTI cruise that occurred in 2017 on board
320 *L'Atalante* R/V (Lebrun and Lallemand , 2017), together with a set of multichannel reflection
321 seismic lines recorded during cruises ANTITHESIS 1 (2013) and 3 (2017) (Marcaillou and
322 Klingelhoefer, 2013; 2016) (Fig. 2). Acquisition parameters for the selected MCS lines include
323 a 3.902 inch³ airgun array source and a 720 channels-6.25m trace spacing streamer ensuring a
324 120-fold coverage. Quality control and binning of the MCS data were performed on board using
325 QCSispeed® and SolidQC® (Ifremer), and processing was performed using GEOVATION®
326 (CGG). Processing sequence includes band-pass (2–7–60–80 Hz) and FK filtering, Spherical
327 divergence and amplitude (gain) correction, predictive deconvolution, three steps velocity
328 analysis and Normal Move-Out (NMO) correction, external mutes, internal mutes and further
329 multiple attenuation by 2D-Surface-Related Multiple Elimination and Radon domain filtering,
330 velocity stack and constant velocity (1500m/s) FK migration.

331 Our data set also includes petroleum seismic data acquired in 2D in the 80's over the Saba
332 Bank and an industrial database on the Saba Bank (Fina 1980; Aladdin 1988). These seismic
333 data, described in Church and Allison (2004), show a lower resolution as compared to those of
334 the GARANTI and ANTITHESIS lines. They allow us, however, to extend our interpretation
335 to a zone that is nowadays closed to seismic investigations. We also benefited from other
336 seismic lines from the “Comité d'Etude Pétrolière et Marine” (CEPM) under the supervision of
337 the “Institut Français du Pétrole et des Énergies Nouvelles” (IFPEN) acquired in the 70's during
338 the Antilles IV cruise (e.g., Bouysse et al., 1985a; b; Bouysse and Mascle, 1994). The seismic

339 stratigraphy of the Saba Bank petroleum surveys was calibrated by using two exploration wells
340 (SBD1 and SBD2; Church and Allison, 2004). The CPEM lines in the vicinity of the Antigua
341 Bank were calibrated using offshore-onshore correlations (Legendre, 2018), wells IODP 340
342 (Coussens et al., 2012) and dredges ARCANTE 1 (Andréïeff et al., 1980).

343 Seismic facies and units are determined following the classical criteria of Mitchum and
344 Vail (1977) and Roksandic (1978).

345

346 **5. RESULTS**

347

348 **5.1. Onshore**

349 **5.1.1. Anguilla**

350 Seven sections of Anguilla (Appendix C) yielded stratigraphically significant taxa of
351 larger benthic foraminifera (Appendix B) and calcareous nannofossils (Appendix A). Based on
352 the identified taxa, we were able to date each of the logged and sampled sections (Fig. 3). Above
353 Paleogene turbiditic beds tilted to the SE (Crocus Bay section; Andréïeff et al., 1988) (Fig. 4A),
354 we found 60 m- thick coral boundstones organized into coral banks and low-relief domes where
355 platy and massive colonies dominate (Fig. 4, B, C, E, F). Associated with the boundstones, we
356 found some bioclastic packstones with abundant corals, larger benthic foraminifera
357 (miogypsinids, amphisteginids, miliolids, and soritids, e.g., *Archaias*), echinoids, red algae,
358 mollusks (pectinids and oysters), and frequent *Teredo* in life position (Fig. 4D). Ten genera and
359 eighteen species of hermatypic corals occur in this platform, among which the *Porites* genus is
360 dominant, the next most abundant being *Montastraea* and *Stylophora* (Budd et al., 1995). Our
361 biostratigraphic analyses indicate that the succession encompasses the Aquitanian to Tortonian-
362 Messinian interval (N4-N18, 23-5.33 Ma) and, except the local occurrence of hardgrounds, no
363 clear evidence of hiatuses has been found in the field. Beds are vertically stacked but low-angle

364 cross-bedded units were found prograding southeastward along the southern coast (e.g.,
365 localities ANG3, 9 and 10) and in the northeastern part of the island (ANG 6) (Appendix C).

366 The Neogene deposits of Anguilla likely correspond to those of an isolated shallow reefal,
367 protected inner platform (Fig. 3), as already suggested by Budd et al. (2005) based on the study
368 of some coral build-ups. This platform contains units with prograding beds towards the SE,
369 indicating that it was opening towards a deeper marine setting.

370

371 5.1.2. *St Martin*

372 Above tilted Paleogene volcanoclastic rocks, the succession of the southwestern part of
373 the island comprises, from bottom to top (Fig. 5; localities in Appendix D):

374 1. **10 to 18 m- thick coral reef boundstones and associated bioclastic packstones** (Fig.
375 6A to C). In the Sabannah area, 4 m- high patch reefs with branching colonies are exposed.
376 Larger benthic foraminifera are mainly represented by miogypsinids and amphisteginids.
377 Planktonic foraminifera (globigerinids) and calcareous nannofossils are also present. At Mullet
378 Bay, we found cross-bedded packstones with red algae and foraminifera and some coral beds.
379 The benthic foraminiferal assemblages are dominated by amphisteginids and *Asterigerina*.
380 Elsewhere, in the Juliana Bay and Kool Hill sections, well bedded bioclastic limestones and
381 coral banks are exposed. Foraminifera are dominated by *Archaias*, *Praerhapydionina*,
382 *Cyclorbiculina*, *Miosorites*, *Androsinopsis* and *Miarchaias*, associated with small miliolids and
383 textulariids. At Kool Hill, karstic cavities infilled by red silty clays and associated with a
384 paleosol level indicate a temporary emersion (Fig. 7C). Our biostratigraphical analyses indicate
385 that the lower part of these deposits correlates with planktonic foraminiferal Zone N5 (latest
386 Aquitanian-early Burdigalian, 21-18 Ma) and the upper part with Zones N6-N8a (late
387 Burdigalian, ~18-15.97 Ma) (Appendix D). The late Burdigalian deposits of the Juliana Airport
388 road section (Fig. 7A) are affected by synsedimentary normal faults (Fig. 7A, B) associated

389 with a local subaerial erosion surface with karstic gullies. Karstic microcaves were found only
390 below this surface, which confirms the existence of a temporary emersion (Fig. 7C-E).

391 2. **31 m- thick bioturbated wackestone with intercalations of packstone and breccias.**

392 The wackestones yielded planktonic and benthic foraminifera as well as red algae. The
393 packstones contain red algae, foraminifera, echinoids and green algae, with some beds
394 organized into hummocky cross-stratification. Some patch reefs with several coral genera
395 locally occur (Fig. 6D). The breccias consist of angular cm- sized debris of coral reef and
396 bioclastic deposits. Planktonic foraminifera indicate that the lowermost part of this sedimentary
397 unit was deposited during the late Serravallian-Tortonian, between 12.8 Ma and 8.2 Ma. Above,
398 foraminiferal assemblages point to Zones N14 to N19 (Tortonian to possibly Zanclean, 11.6-
399 3.8 Ma). The foraminifera in the uppermost part of the section point to Zone N19 and were
400 deposited during the Zanclean, between 5.33 Ma and 3.8 Ma. The perireefal blocks of the
401 breccias originated from two different sources: some developed laterally to patch reefs (Fig.
402 6D); others were eroded from the underlying late Burdigalian coral complex. Langhian to lower
403 Serravallian deposits were not identified in St Martin, which could then indicate a depositional
404 hiatus.

405 3. **1 to 3 m- thick cross-bedded packstone with red algae and foraminifera**, resting on
406 a subaerial erosive surface (Fig. 6E). The foraminifera found in these deposits point to Zone
407 N19 (Zanclean, 5.33-3.8 Ma).

408 In the southwestern part of St Martin, the Aquitanian-Burdigalian deposits comprise
409 different depositional settings (Fig. 5). To the West (Terres Basses), we found high-angle
410 dipping coral rubble beds overlain by low-angle dipping coral build-ups. This area is interpreted
411 as the outer slope of a coral system, probably set up on the flanks of a late Oligocene subaerial
412 volcano. In the Sabannah area, the occurrence of m- high patch reefs with branching colonies,
413 planktonic and benthic foraminifera, is interpreted as a reef to foreef zone in an open sea

414 (BouDagher-Fadel, 2008; Montaggioni and Braithwaite, 2009). At Mullet Bay, packstones with
415 red algae and benthic foraminifera (amphisteginids and *Asterigerina*) and some coral beds and
416 crossbedding occur, indicating inner-ramp, reefal deposits. In the Juliana Bay and Kool Hill
417 sections, coral banks and benthic foraminiferal assemblages are indicative of a quiet lagoonal
418 depositional environment (Andréieff et al., 1988; Tucker and Wright, 1990; BouDagher-Fadel,
419 2008). To the east of St Martin, the data of Andréieff et al. (1987; 1988) indicate the presence
420 of coral reefs at Pinel Islet and on islets east of Phillipsburg. As a result, St Martin was an island
421 during the early Miocene, bordered by coral reef formations with lagoons to the southeast and
422 fringing reefs to the northeast. Langhian deposits were not found, suggesting a possible middle
423 Miocene emersion. Deposition of the upper Serravallian–Tortonian sediments of St Martin
424 (Cupecoy) first occurred in a mid-outer-ramp environment above the Burdigalian reefal
425 deposits indicated by abundant pelagic microfossils. These deposits change upward into mid to
426 inner ramp settings with coral patch-reefs, and associated reefal breccias during the Messinian
427 and the early Zanclean. Zanclean erosional surfaces affect the deposits, indicating a shallowing
428 upward trend ending with an emergence. In this area, the occurrence of reworked breccias from
429 Burdigalian reefal deposits testifies for and indicates the permanence of emerged areas.

430

431 5.1.3. *Tintamarre*

432 At Tintamarre, the deposits are dominated by clayey limestones that yielded abundant
433 macrofauna and larger benthic foraminifera dominated by *Lepidocyclina*, *Miolepidocyclina*,
434 *Miogypsina* and *Amphistegina* associated with planktonic foraminifera. On the basis of six
435 outcrops (Appendix E), the succession comprises, from bottom to top (Fig. 8):

436 1. **13 m- thick packstones** with bivalves (oysters, *Amusium*, *Chlamys*), echinoids
437 (*Clypeaster* and scutellids), larger benthic foraminifera, and some coral debris. The microfossils
438 from the upper part of this unit correlate with the early part of Zone N8 (late Burdigalian);

439 2. **11 m- thick matrix-supported lower megabreccia** with reefal to perireefal clasts
440 (Appendix D; Fig. 9A). Clasts are cm to m- sized with blocks reaching 3 m wide, embedded
441 into a lime wackestone matrix displaying slump structures and forereef-derived bioclasts
442 (*Clypeaster*, larger benthic foraminifera, red algae, and molluscs). Reworked blocks do not
443 display emersion features;

444 4. **0 to 4 m- thick brown clays with gypsum crystals.** This facies, found only in the TINT
445 10 locality on the northern coast of the island laterally pinches on top of the megabreccia
446 (Appendix D). The three previously described units are yellow to orange in the field, locally
447 brown;

448 5. **33 m- thick wackestone with packstone and breccia interbeddings.** Wackestones
449 mostly yielded bivalves (*Amusium* and other pectinids), echinoids (*Clypeaster*, scutellids), and
450 benthic foraminifera. Packstones are unsorted, mm- to cm- grain-sized, debris-flows with well-
451 preserved pieces of corals, red algae and molluscs. A hummocky cross-stratification is locally
452 found into the packstones. The breccia is composed of cm- grain-sized reworked reefal to
453 perireefal limestones. The succession is tilted to the SE below an erosional surface (Appendix
454 E). The lower 19 m of the lithological succession is green and contains microfossils pointing to
455 Zones N6-N8 (late Burdigalian, 18-15.97 Ma); the upper 14 m is white and microfossils point
456 to Zones N8-N11 (Langhian, 15.9-13.6 Ma).

457 6. **Up to 11 m- thick calcareous upper megabreccia** (Fig. 10). This megabreccia rests
458 unconformably on an erosional surface that transects previously tilted deposits (Appendix E).
459 It is composed of dm- to m- sized transported blocks of coral reef and associated bioclastic
460 deposits and rafted red algae and coral limestone beds reaching several tens of meters long and
461 up to 5 m- thick (Appendix E; Fig. 9A, B). The blocks are embedded into a white to pink
462 wackestone matrix. The megabreccia is crosscut by shear zones and displays numerous soft
463 sediment structures, slump, recumbent folds, isoclinal folds and balls and pillows (Fig. 9C;

464 Appendix E). Shear zones and slumps are indicative of a transport direction to the S-SE. The
465 reefal and red algal-coral rafted beds and clasts yielded benthic foraminiferal assemblages of
466 Zones N5-N8a (latest Aquitanian-Burdigalian; e.g., samples CSM 42, 70 and 71; Appendix E).
467 The matrix yielded planktonic foraminifera further indicating Zone N8b (early Langhian, 15.4-
468 15 Ma). Consequently, the upper megabreccia deposited during the early Langhian and
469 comprises reworked Burdigalian limestones.

470 In Tintamarre, Burdigalian to lower Langhian deposits are dominated by clayey limestones
471 that provided shallow-water fauna and debris flow interbeddings with transported corals. Two
472 megabreccias with rafted beds and slumps also occur. The depositional setting is interpreted as
473 an open sea, muddy forereef slope testified by abundant and well-preserved coral fragments
474 (Fig. 8). During the late Burdigalian, however, lagoon conditions temporarily existed with the
475 deposition of gypsum clays above the lower megabreccia. This indicates that the forereef slope
476 depositional setting temporarily turned to shallower conditions then. The upper megabreccia
477 comprises Burdigalian debris and rafts, which were emplaced in a muddy forereef environment
478 during the early Langhian (15.4-15 Ma) (Appendix E; Fig. 9). This megabreccia unconformably
479 lies upon southeastward tilted and eroded early Langhian beds. The blocks of the upper
480 megabreccia do not display any emergence or tectonic features. This indicates that both their
481 destabilization and transportation have occurred under submarine conditions, as classically seen
482 in submarine active tectonic settings where large scale mass wasting is reported (e.g., Hine et
483 al., 1992; Zachariasse et al., 2008; Dailey et al., 2019). The upper megabreccia was transported
484 towards the ESE to SE, indicating that it originated from the WNW to NW in the submerged
485 part of the Burdigalian reefal platform of Anguilla. One way to explain this arrangement is to
486 consider that normal faults trending NE-SW and deeping NW occurred at that time between
487 Anguilla and St Martin, this type of fault having been identified in the southwestern part of St
488 Martin (Legendre, 2018).

489

490 5.1.4. *Barbuda*

491 The Highland Fm. comprises a 30 m- thick carbonate succession. The lower part of
492 the formation does not crop out. From bottom to top we identified (Appendix F):

493 1. **4.5 m- thick grainstones with isolated massive, coral colonies.** Corals are dominated
494 by *Montastraea* and *Porites*. The sediments yielded benthic foraminifera (*Miarchaias*, and
495 *Amphistegina*) pointing to the late Miocene;

496 2. **9 m- thick red algal and larger benthic foraminifera-rich wackestones to**
497 **packstones;**

498 3. **3.5 m- thick wackestones with some isolated coral colonies** and benthic and
499 planktonic foraminifera (*Neogloboquadrina acostaensis*, *Sphaeroidinellopsis subdehiscens*,
500 and *Globorotalia margaritae*) indicative of a Zanclean age;

501 4. **12.5 m- thick red algal wackestones to packstones with benthic and planktonic**
502 **foraminifera.** The uppermost part of the succession is severely weathered. Planktonic
503 foraminifera indicate that the lower and upper parts of the unit was deposited during the
504 Zanclean and between the Zanclean and Piacenzan, respectively.

505 In Barbuda, benthic foraminifera are dominated by amphisteginids. Mud and planktonic
506 foraminifera occur throughout the section. Corals are documented as isolated, and consist of
507 massive colonies in life position. Consequently, the depositional environment is interpreted as
508 an open-sea, shallow water reefal to forereef muddy carbonate platform or ramp deposited in
509 low-energy conditions. These results are in agreement with those of Brasier and Donahue
510 (1985), who estimated a palaeobathymetry of *ca* 40-50 m. The middle part of the section is
511 dominated by planktonic foraminifera facies devoid of corals, indicating a deeper environment
512 of deposition than the lower and upper parts of the section. This suggests that the succession
513 has recorded a regressive-transgressive cycle (Appendix F). During the late Miocene-Zanclean

514 interval (samples BAR 1 to 9; Appendix F), the depositional environment changes from reefal
515 inner-ramp (*ca* 10-20 m palaeodepth) to outer-ramp (*ca* 40-50 m paleodepth). The maximum
516 palaeodepth is reached between samples BAR 9 and 13 and occurred during the Zanclean, when
517 wackestones with abundant planktonic foraminifera were deposited. Above, outer-ramp
518 environment changes into mid-ramp during the Zanclean-Piacenzan (?), thereby indicating a
519 moderate regressive trend.

520 *5.1.5. Antigua*

521 The lowest marine limestone beds of the Antigua Fm. yielded Rupelian foraminifera
522 (*Eulepidina undosa*, *Lepidocyclina* (L.) *yurnagunensis*) (Appendix G), while the limestones
523 above them contained Chattian foraminifera (*Lepidocyclina* (*Lepidocyclina*) *yurnagunensis*, L.
524 (*Nephrolepidina*) *braziliana*, *Heterostegina israelskyi*, and *Neorotalia* sp.) (e.g., Pares cross-
525 section; Appendix G.). Consequently, the Antigua Fm. is likely to have been deposited between
526 the Rupelian and the Chattian.

527 In Antigua, the Central Plain Group was deposited into lakes and coastal lagoons, as
528 previously documented (e.g., Martin-Kayes, 1959; Frost and Weiss, 1979; Donovan et al.,
529 2014). Above, the Antigua Fm. was deposited along a low-angle northeastward dipping
530 carbonate ramp, with inner-ramp, reefal environments in the southwest changing
531 northeastwardly into a mid-ramp depositional setting characterized by abundant planktonic
532 foraminifera. These results are in agreement with the regional sedimentary organisation
533 proposed by Martin-Kaye (1969).

534

535 *5.2. Offshore*

536 The profiles GA 11, GA 15, ANT019-24, CPEM 302, CPEM 509 and CPEM 510 are
537 used to compare onshore data with offshore ones because: 1) GA 15 intersects the seismic
538 profile C2 of the Saba Bank petroleum prospect, which was calibrated using wells SBD1 and

539 SBD2 (Matchette-Downes, 2007); 2) GA 11 allows following seismic sequences to the north
540 across the Kalinago Basin; 3) ANT019-24 allows investigating the northwestern margin of the
541 Anguilla Bank; 4) CPEM 302 provides information about the southern part of the Anguilla
542 Bank and allows correlations with the southern part of the Kalinago Basin; and 5) CPEM 509
543 and CPEM 510 illustrate the seismic stratigraphy of the Antigua Bank. In addition, the northern
544 ends of lines GA 08 and GA 09 are only 5 km away from the island of St Martin (Appendix J),
545 213A was performed on the Anguilla Bank south of St Barthélemy (Appendix J), and 509-510
546 are located in the vicinity of the island of Antigua, allowing onshore-offshore correlations.

547

548 *5.2.1. Seismic sequences*

549 We identified seven seismic megasequences bounded by regional prominent
550 unconformities and their correlative conformities (Vail et al., 1977; van Wagoner et al., 1988;
551 Cattuneanu, 2006) over the whole investigated area (MS1 to MS7). The most complete
552 succession is best exemplified south of the Saba Bank, along crossing lines GA 15 (ENE-WSW;
553 Fig.10A) and Saba Bank C2 (NW-SE; Fig. 10B). The C2 line was reinterpreted and a seismic
554 pattern partly similar to that of Church and Allison (2004) was found, thereby allowing
555 chronostratigraphic assignments to the megasequences. From bottom to top they are:

556 - **Megasequence 1 (MS1)**: it comprises poorly-defined, chaotic reflectors, locally overlaid by
557 low to very low frequency, discontinuous reflectors. Transparent facies also occur. The top of
558 the sequence is an erosional unconformity termed SB1 usually underlined by a strong amplitude
559 reflection. In wells SBD1 and SBD2, MS1 is overlaid by a subaerial andesitic lava flow that
560 occurred during the late Eocene (38.1-35.9 Ma interval; Church and Allison, 1984). MS1 is
561 found on the GARANTI and ANTITHESIS lines (Figs. 10 to 12; Appendix J) and on the CPEM
562 lines, especially in the southern part of the Kalinago Basin (Fig. 13).

563 No accurate information about MS1 is available yet. Nevertheless, reworked Cretaceous
564 and Paleocene microfossils have been found in the overlying megasequence MS3, suggesting
565 that MS1 is partly made of sedimentary rocks of these ages.

566 - **Megasequence 2 (MS2)**: it comprises seismic units displaying inverted half-graben structures
567 with faint and subparallel to fan-shaped reflectors (Fig. 10A and B). In some cases, it is
568 organized into fan-shaped reflectors draping underlying topographic highs and thickening
569 downward (Fig. 11A; 12). The half-grabens are visible on NE-SW profiles (fig. 10B) and not
570 on NW-SE profiles (Fig.10A), suggesting that their orientation is overall NW-SE. MS2 has not
571 been reached by the drillings. The top of MS2 is the irregular, erosional, newly defined surface
572 SB2 found extended below the late Eocene subaerial andesite drilled in the Saba Bank (Church
573 and Allison, 1984). MS2 has not been recognized in the southern part of the Kalinago Basin
574 (Fig. 13). MS2 probably consists of sedimentary deposits lying unconformably on MS1 (Figs.
575 10A, 11A). It underwent a late mid-Eocene compression leading to inversion of half grabens
576 (Philippon et al., 2020a).

577 - **Megasequence 3 (MS3)**: it comprises up to 2.5 second two-way travel-time (stwt)- thick
578 deposits. MS3 is characterized by discontinuous to continuous reflectors of low amplitude,
579 medium to high frequency, always sub-parallel and well stratified, locally prograding (Fig. 10).
580 MS3 onlaps above SB2 and seals the compressive deformations in MS2. It is marked by an
581 abrupt change in seismic facies that evolves from continuous well-bedded reflectors, low-angle
582 truncations in MS2 to onlaps in MS3. The top of the sequence is covered by an unconformity
583 hereafter named SB3. MS3 was not identified in the southern part of the Kalinago Basin (Fig.
584 13).

585 In the northern part of the Kalinago Basin, MS3 displays regular, mid-amplitude and
586 parallel reflectors (Fig. 10) that progressively pinch against spurs (Fig. 10A, 11A). On lines
587 GA-08 and 09, MS3 displays prograding beds on the southern margin of the Anguilla Bank, a

588 pattern that is also found on lines ANT 19 and 24 (Fig. 11B; Appendix J). These prograding
589 beds are related to downslope detritus originating from the topographic highs. Along the flanks
590 of the spurs, the beds of MS3 are organised into fans mimicking the shape of the relief and
591 down-lapping above unconformity SB2, controlled by NW-SE trending syn-sedimentary faults
592 (Figs. 11A and 13; Appendix J). On the Walichi Flat, south-southwestward prograding beds
593 develop above the basement (Fig. 12B). Offshore in the Antigua Bank and the southern part of
594 the Kalinago Basin, MS3 is missing (Fig. 14). Onshore, continental deposits are recorded
595 (Central Plain Group of Antigua). These observations indicate that the Kalinago Basin was not
596 extending in this area (Fig. 13). Consequently, MS3 has been deposited into sub-basins
597 separated by topographic highs. As no recent fault was evidenced on the margins of the
598 Kalinago Basin, the difference of elevation between the top of the Anguilla Bank and the MS3
599 deposits of the Kalinago Basin varies between 1,000 to 1,500 m, broadly reflecting the
600 palaeobathymetry of the deep parts of the basin. Such a difference in elevation is also found in
601 the southeastern part of the Saba Bank (Fig. 10).

602 In summary, MS3 unconformably resting upon the erosional surface SB2 is characterised
603 by high relief changes with topographic highs (Walichi Flat, Saba Bank, and spurs) and newly-
604 formed depocentres controlled by syndimentary normal faults (northern Kalinago Basin).

605 - **Megasequence 4 (MS4)**: it comprises up to 2.5 stwtt- thick gently-dipping reflectors, locally
606 organized into low angle inclined prograding units (Figs. 10 to 12). Onlaps are present against
607 paleoreliefs (Appendix J). The sequence ends with an erosional surface termed SB4 that
608 truncates the underlying reflectors. Locally, low angle reflectors of the overlying megasequence
609 onlap onto SB4. Opposite to MS3, MS4 occurs regionally, from the Kalinago Basin in the NW
610 (Figs. 11, 12) to the Antigua Bank in the SE (Fig. 13).

611 Northeast of Saba Bank, deposition of MS4 is controlled by syndimentary faults in
612 the NW-SE direction. (Fig. 11A). Southeast of the Saba Bank, MS4 displays parallel bedding

613 (Fig. 10) or fans (Fig. 11A), above the unconformity SB3. In the vicinity of the submarine spurs
614 (Anguillita, Southeastern seamounts) and highs (Saba Bank, Anguilla Bank, and Walichi Flat),
615 SB3 is erosional with toplaps in the underlying MS3 and onlaps in the overlying MS4 (Figs,
616 10, 11, 13; Appendix J). In the southern part of the Kalinago Basin and Antigua Bank, MS4
617 directly overlies MS1. Consequently, MS4 is deposited on a topographic surface SB3 which is
618 erosional, except in the deepest parts of the depressions. SB3 exhibits an erosive character over
619 *ca* 500 m vertical drop at maximum, and consequently sedimentation in troughs occurred at
620 several hundred meters depth.

621 - **Megasequence 5 (MS5)**: it reaches 1 stwtt- thick and comprises medium to strong amplitude,
622 medium frequency, parallel continuous reflectors. The sequence shows an aggrading pattern
623 and retrogrades on older reliefs. The top of MS5 is characterised by an unconformity termed
624 SB5. SB5 is either erosional (Fig. 10A, northern part) or bedding is sub-parallel with low-angle
625 onlaps above (Fig. 10B, Saba Bank). MS5 is found from the Kalinago Basin in the NW (Fig.
626 11, 12) to the Antigua Bank in the SE (Fig. 13).

627 In the Kalinago Basin, South of the Saba Bank, Walichi Flat and Antigua Bank, MS5 is
628 organised into parallel reflectors mostly parallel to MS4 reflectors. Onlaps are found in the
629 vicinity of submarine highs, above SB4. The latter displays clear erosional features on the spurs,
630 on the margin of the Anguilla Bank, on the Walichi Flat and on the uppermost part of the Saba
631 Bank (Figs. 10, 11, 12). Consequently, SB4 is interpreted as a subaerial structure developed on
632 submarine highs, that is confirmed by the analysis of the dredged GA 03 rock-samples collected
633 on the southeastern spur (Fig. 2; Appendix I; see below). Erosion is found over a few hundred
634 meters depths at maximum, suggesting that deposition of MS5 occurred at several hundred-
635 metres depth in basin areas.

636 - **Megasequence 6 (MS6)**: it reaches 0.5 stwtt- thick and comprises medium- to strong-
637 amplitude, medium-frequency, continuous and parallel reflectors and prograding reflectors. On

638 the Saba Bank, reflectors are parallel and strongly reflective (Figs. 10, 11), like on the Anguilla
639 Bank and the Antigua Bank (Fig. 13). In the southern part of the Kalinago Basin, MS5 is locally
640 overlain by an erosional surface termed SB6.

641 - **Megasequence 7 (MS7)**: it is distinguishable in the southern part of the Kalinago Basin and
642 Antigua Bank on CPEM seismic lines (Figs. 2, 13). It comprises medium- to strong- amplitude,
643 medium-frequency, continuous and parallel reflectors which locally display fan shaped
644 structures. In the northern part of the investigated area, SB6 is parallel to reflectors and both
645 MS6 and MS7 are often indistinguishable. Consequently, they are grouped into a MS6+MS7
646 megasequence (Fig. 10).

647 In most of the investigated area, deposits of MS6 and MS7 conformably cap those of
648 MS5. Erosional features are found in the vicinity of spurs (Anguillita and Martinita seamounts)
649 and on Walichi Flat where SB5 displays truncations of the underlying MS5 (Fig. 11). Discrete
650 onlaps of fan-shaped reflectors of MS7 above SB6 are found in the southern part of the Kalinago
651 Basin, partly related to the syndimentary activity of recent normal faults (Fig. 13).

652

653 5.2.2. *GARANTI dredged samples*

654 Dredged samples have been collected on the flanks of seamounts in the northwestern part
655 of the Kalinago Basin and are localized on seismic profiles to allow calibrating the seismic
656 stratigraphy (Fig. 2): DR GA-04-01 and DR GA-04-02 are located on the seismic profile GA11
657 and DR GA-03-01 on GA13.

658 Dredge DR GA-04-01 (Fig. 11), in MS6, yielded bioclastic wackestones to packstones with
659 red algae and benthic foraminifera. Larger benthic foraminiferal assemblages in these samples
660 correlate with the planktonic foraminiferal zones N14-N18, thus indicating a late Miocene age
661 of deposition (Appendix I).

662 Dredge DR GA-04-02 (Fig. 11), in MS6, yielded wackestones and packstones with
663 planktonic foraminifera. One sample point to Zones N18-N19 (latest Messinian-Zanclean, 5.8-
664 3.8 Ma), when another points to Zone N19 (Zanclean, 5.33-3.6 Ma). The wackestones with
665 planktonic foraminifera are bored and borings are infilled with likely modern muds containing
666 planktonic foraminifera of Zones N22-N23 (Calabrian-Holocene).

667 Dredge GA-03-01 in MS5 yielded packstones with red algae and foraminifera pointing to
668 Zones N12b-N20a (Serravallian-Zanclean). The packstones have suffered from
669 microsparitization and are crosscut by opened fractures infilled with wackestones enriched in
670 planktonic foraminifera and reworked microsparitized red algal packstones (Appendix I). The
671 foraminifera found within the wackestones infillings point to Zone N19 (Zanclean).

672

673 **6. DISCUSSION**

674

675 **6.1. Age model**

676 *6.1.1. Onshore*

677 In the Anguilla Bank, the synthetic lithostratigraphical succession of each island can be
678 reconstructed and correlated based on our new biostratigraphic data and field investigations
679 (Fig. 14). In the three islands of the Anguilla Bank, the age of the lower part of the Neogene
680 reefal deposits ranges between the (late?) Aquitanian and the Burdigalian. This age is consistent
681 with i) our new radiometric data at *ca* 25-24 Ma (latest Oligocene) of the andesitic boulder from
682 submarine lahar deposits found below the carbonate platform in St Martin (Appendix K) and
683 ii) that of a subaerial lava flow found in St Barthélemy in a similar setting (Legendre et al.,
684 2018; Cornée et al., 2020) (Appendices G and H). Middle Miocene (Langhian-Serravallian)
685 deposits occur in Anguilla and Tintamarre, but they are missing in St Martin where an erosional
686 unconformity is strongly suspected to have occurred between the Burdigalian and the

687 uppermost Serravallian-Tortonian deposits. However, outcrop conditions did not allow direct
688 observation of this surface. Late Miocene (Tortonian-Messinian) sediments were found in St
689 Martin and Anguilla. In Tintamarre, they may have deposited, but were probably removed by
690 erosion. Zanclean deposits have been identified in St Martin where they are transected by
691 erosional surfaces.

692 In the Antigua Bank and Barbuda, the Highland Fm. encompasses the late Miocene-
693 Piacenzan interval at youngest (Appendix F). Neither unconformity nor major facies change
694 were found between the upper Miocene deposits (samples BAR 1 to BAR 7) and the overlying
695 Zanclean ones. Consequently, a latest Miocene age is considered here (Messinian) for the lower
696 part of the Highland Fm. In Antigua, sediments of the Central Plain Group deposited during the
697 Rupelian (because they are located below the Antigua Fm.), and those of the Antigua Fm.
698 deposited between the Rupelian and the Chattian (Appendix G).

699

700 *6.1.2. Offshore-onshore correlations*

701 Age calibration of offshore sequences and unconformities takes into account the
702 calibration of line C2 with Saba Bank wells, correlations through seismic sequences and
703 unconformities, and dredges data from the GARANTI and other cruises (Fig. 2). These
704 combined data allow calibrating the seismic stratigraphy, correlating onshore and offshore
705 sequences and concur to constrain a late Eocene-Pleistocene age range for the deposits of the
706 Anguilla Bank, Antigua Bank, and Kalinago Basin (Fig. 15).

707 • **MS1:** it correlates with the acoustic basement overlain by a subaerial andesitic complex
708 or MS2. The only chronostratigraphic data available indicate ages ranging between 38.7 Ma
709 and 30.8 Ma (Priabonian–Rupelian) in the Saba Bank wells (Church and Allison, 2004;
710 Matchette-Downs, 2007). The wells did not reach nor MS1 neither MS2 but yielded reworked
711 Cretaceous and Paleocene microfossils in the sequences overlying the subaerial andesitic

712 complex. Following Jany et al. (1990) and Church and Allison (2004), MS1 is considered to
713 have been deposited between the Late Cretaceous and the middle Eocene.

714 • **MS2:** this locally folded unit (Philippon et al., 2020a) (Fig. 10A) was previously
715 included into the acoustic basement of Church and Allison (2004). It is located between the
716 basement and the Priabonian-Rupelian andesites of wells SBD1 and SBD2, and the overlying
717 megasequence MS3 dating from the late Eocene-early Oligocene. On land at St Barthélemy,
718 compressive structures affecting middle Eocene carbonate deposits (Cornée et al., 2020) have
719 been estimated to have occurred during the late middle-Eocene (Philippon et al., 2020a).
720 Consequently, MS2 and SB2 are assigned to the early middle-Eocene.

721 • **MS3:** it corresponds to the “Lower Carbonate Unit” and the “Channel Turbidite Unit”
722 of Church and Allison (2004) identified on the re-interpreted profile C2 (Fig. 10B). Based on
723 foraminiferal data, the “Lower Carbonate Unit” points to the late Eocene in well SBD1. Based
724 on calcareous nannofossils, the “Channel Turbidite Unit” has been dated to the late Eocene-
725 early Oligocene interval in well SBD2 (Church and Allison, 2004). Consequently, MS3 has an
726 age ranging from the late Eocene to the early Oligocene.

727 • **MS4:** it corresponds to the “Fluvial Deltaic Unit” of Church and Allison (2004) on
728 profile C2 (Fig. 11). This unit yielded microfossils ranging in age from the late Oligocene to
729 the early Miocene (Church and Allison, 2004). On profile GA 08, MS4 can be traced to 5 km
730 off St Martin (Fig. 2; Appendix J). There, MS4 displays progradations and chaotic reflectors.
731 Onshore in St Martin, the margin of the early Miocene carbonate platform is marked by forereef
732 slope deposits which exhibit high dip. (Fig. 6A-B). Moreover, an Oligocene subaerial
733 unconformity was also found in St Martin (Andréïeff et al., 1988; this work) and St Barthélemy
734 (Cornée et al., 2020), between late Eocene and early Miocene deposits. In the Antigua Bank,
735 MS4 partly correlates with the Rupelian-Chattian Oligocene Antigua Fm. Consequently, MS4

736 deposited during the late Oligocene-early Miocene interval, and the underlying unconformity
737 SB3 is Oligocene.

738 • **MS5:** it corresponds to the lower part of the Upper Carbonate Unit. Foraminifera and
739 calcareous nannofossils indicate that its lower part is not younger than the early Serravallian
740 and its upper part Zanclean at youngest (Church and Allison, 2004). The basal unconformity
741 SB4 is assigned to the middle Miocene and can be traced up to the margin of the Anguilla Bank
742 (lines CPEM 302, GA 08, GA 09; Appendix J). Onshore in St Martin and Tintamarre, this
743 middle Miocene (Langhian) unconformity also occurs, and is overlaid by late Serravallian to
744 Zanclean deposits (Fig. 14). In V-shaped basins eastward in the forearc, Boucard et al. (2021)
745 also described a regional erosional unconformity UB2 between early and middle Miocene
746 sedimentary units. Consequently, MS5 is assigned to the middle-late Miocene and the
747 underlying SB4 unconformity was possibly emplaced during the Langhian.

748 • **MS6:** it corresponds to the upper part of the “Upper Carbonate Unit” of Church and
749 Allison (2004). In the Saba Bank wells, this sequence provided bioclastic coral-dominated
750 deposits covering a red-algal dominated platform. MS6 rests on the erosional unconformity
751 SB5, which corresponds to the base of the reefal deposits still remaining undated. The haul-
752 dredges carried out during the cruise GARANTI on the Martinita and Southeastern seamounts
753 within MS5 and MS6 (Figs. 2 and 11), yielded upper Miocene and lower Pliocene limestones
754 (DR GA 03-01, 04-01, and 04-02; Appendix I). Because microsparitization is found in the upper
755 Miocene limestones, which are also affected by open fractures infilled with Zanclean deposits,
756 we conclude that the Martinita and Southeastern seamounts emerged during the latest Miocene
757 at oldest, and that they subsequently started drowning during the Zanclean. This emersion could
758 relate to SB5. Moreover, the lower Pliocene limestones at site DR-04-02 exhibit borings that
759 may indicate that the seamounts were very near sea level or emergent during the Piacenzan-
760 Gelasian interval and were drowned by the Calabrian. These borings could relate to SB6

761 unconformity. In St Martin, erosional unconformities are found in lower Zanclean deposits (Fig.
762 6E). In the Guadeloupe Archipelago (*ca* 250 km further south), there is a shallow water
763 carbonate platform that was deposited above a major, latest Miocene to early Pliocene,
764 erosional unconformity (Cornée et al., 2012; Münch et al., 2014; De Min et al., 2015). Red
765 algae-rich deposits dominate in its lower part (Zanclean-Gelasian), and gradually change
766 upwards to coral-dominated deposits (Gelasian-Calabrian). This succession is similar to MS6
767 in Saba Bank wells. In the Antigua Bank, MS6 was also partly correlated with the Zanclean-
768 Calabrian deposits recovered from the IODP leg 340 (Legendre, 2018). Consequently, the
769 underlying SB5 unconformity is confidently assigned to the latest Miocene-early Pliocene, and
770 MS6 to the early Pleistocene.

771 • **MS7**: it mainly occurs in the southern part of the Kalinago Basin where it is thick enough
772 to be identified on seismic profiles. The wells recovered from IODP 340 indicate a Calabrian
773 (1 Ma) to Holocene age (Coussens et al., 2012). In the northern part of the Kalinago area, MS7
774 remains thin and was grouped with MS6.

775 In summary, offshore and onshore data allow us to date the Cenozoic deposits in the
776 northern Lesser Antilles, assigning ages to the regional unconformities and estimating the
777 duration of their corresponding hiatuses (Fig. 15): SB1 was emplaced during the Paleocene to
778 middle Eocene ; SB2 during the late Eocene; SB3 during the Oligocene; SB4 during the middle
779 Miocene (Langhian); SB5 during the latest Miocene-early Pliocene; and SB6 during the early
780 Pleistocene.

781

782 **6.2. Palaeogeographical evolution**

783 Using our dataset that combines onshore and offshore investigations and correlations,
784 we are able to propose novel palaeogeographical maps of the Northern Lesser Antilles (Fig.
785 16). Sequence boundaries on seismic lines were considered subaerial when regional erosional

786 features were observed, with the following criteria: clearly-identified toplaps and onlaps below
787 and above the unconformities, respectively.

788 During the Eocene, the Anegada Passage did not exist (Jany et al., 1990; Mauffret and
789 Jany, 1990). The upper Eocene SB2 unconformity, following an upper Eocene compression
790 (Philippon et al., 2020a), is regionally erosive. MS2 is only preserved as relict patches in the
791 northern part of the Kalinago Basin, Saba Bank and Anguilla Bank, suggesting that SB2 is the
792 expression of a general emersion. The emerged area was extended from the Saba Bank to the
793 Antigua Bank, for at least 300 km, and was connected to Puerto Rico (GraNoLa landmass of
794 Philippon et al., 2020a). In the Anguilla Bank, late Eocene sedimentation resumed after SB2,
795 linked to volcanic activity in St Barthélemy.

796 During the latest Eocene-early Oligocene (MS3) (*ca* 38-28 Ma), to the north of the
797 studied area, a major extensional episode occurred along NW-SE trending faults. The Kalinago
798 Basin opened and the sea invaded the depressions despite the sea level drop of about a hundred
799 meters that occurred at the Eocene-Oligocene transition (Miller et al., 2020). The Saba,
800 Anguilla and Antigua banks and the Walichi Flat remained all above sea level in the footwall
801 of normal faults. At that time, volcanism was active in Antigua, St Martin and St Barthélemy
802 islands, and in Saba Bank (Fig. 16B).

803 During the late Oligocene (SB3) (28-23 Ma), the rifting propagated southward and the
804 Kalinago Basin deepened. Its eastern and western shoulders were uplifted and became emergent
805 in the Saba Bank and from Antigua to the Walichi Flat (Fig. 16C). Onshore, this emergence is
806 clearly recorded: in St Martin, subaerial upper Oligocene volcanism is now proven and
807 Aquitanian reefs developed onto tilted and eroded Eocene sediments (Andréieff et al., 1988;
808 this study); in St Barthélemy, an erosional surface crosscutting the upper Eocene deposits is
809 capped by upper Oligocene subaerial lavas (Cornée et al., 2020); in Antigua, the Rupelian

810 Central Plain Fm. was deposited in an inland paleoenvironmental setting, then the sea invaded
811 the island during the Rupelian and the Chattian.

812 During the latest Oligocene-early Miocene (MS4) (24-16 Ma), only small islands
813 remained above sea-level, despite hundred meters sea level drops, indicating a significant and
814 general subsidence (Fig. 16D). The now drowned but previously emerged area extending from
815 Antigua to Anguilla was then capped by reefal carbonate deposits delineated by steep slopes
816 and their associated deposits. Elsewhere, basin sediments were deposited. Some tectonic
817 activity is recorded in the Anguilla Bank with mass wasting and synsedimentary normal faults
818 in St Martin (Legendre, 2018; this study). A subaerial volcanic activity is evidenced in St
819 Barthélemy and Antigua. Offshore, MS4 infilled depressions or fringes spurs, indicating
820 regional subsidence. Fault activity is recorded only to the north of the study area, on the
821 southern margin of the Walichi flat, in the Kalinago Basin. In the forearc to the east of the
822 Anguilla Bank, steep NE-SW trending fault controlled basins opening (V- shaped basins,
823 Boucart et al. (2021)) (Fig. 1B) (St Barthélemy and Antigua valleys). NW-SE and their
824 conjugated NE-SW trending normal faults were sealed by MS5 (Fig. 10A). In St Martin, the
825 upper Oligocene pluton and its country rock are tilted along NE-SW trending faults (Legendre,
826 2018). In Anguilla, the Eocene beds were tilted to the SE and capped by a sub-horizontal
827 Miocene carbonate platform, suggesting that the tilt was also controlled by this set of NE-SW
828 trending faults. Consequently, moderate fault activity is found only in the northern part of the
829 investigated area, at the vicinity of the Anegada Trough, which probably started to open.

830 At St Martin in the Juliana airport section (Appendix D), E-W trending synsedimentary normal
831 faults affected the upper Burdigalian lagoonal deposits. These faults display dip-slip kinematics
832 indicating a NNE-SSW extension (Fig. 7) (Legendre, 2018; Noury et al., 2018). Such an
833 orientation is consistent with the Kalinago rift trend. Local uplifts have been recorded during
834 this tectonic episode, at Juliana and Kool Hill, with the occurrence of karstic features (Appendix

835 D). In Tintamarre, the lower megabreccia also was deposited during the late Burdigalian (Fig.
836 9; Appendix E), and it was likely coeval with the deposition of lagoonal sediments indicative
837 of a temporary uplift (Fig. 14). Consequently, the emplacement of the lower megabreccia is
838 most related to observed strain affecting the Juliana section, both indicating moderate N-S to
839 NNE-SSW extension (*i.e.* parallel to the trench extension) in this area between 18 Ma and 16
840 Ma.

841 During the early Langhian (SB4) (15.4-15 Ma), the sea level rose by 80 m (Miocene
842 climatic optimum; Miller et al., 2020; Westerhold et al., 2020). Large islands, however,
843 emerged and shallow banks were deposited. This indicates that another significant uplift event
844 occurred, which was most probably controlled by NE-SW faults that tend to be parallel to the
845 Anegada Trough (Fig. 16E). Antigua, southern Anguilla and Saba Banks became emergent
846 whilst the northern Anguilla Bank remained under shallow waters. Elsewhere, basin sediments
847 have been deposited. East of Anguilla Bank, the spurs separating the V- shaped paleovalleys
848 emerged during the early-middle Miocene and underwent erosion (Boucard et al., 2021).
849 Volcanic activity is not recorded onshore neither offshore.

850 Between the middle Miocene and the early Pliocene (MS5) (*ca* 15-4 Ma), a new regional
851 drowning occurred and only small islands were emergent (St Barthélemy and St Martin) (Fig.
852 16F). From Anguilla to Antigua, shallow water reefal platforms have formed whilst basin
853 deposits occurred elsewhere and the V- shaped basin did not operate anymore (Boucard et al.,
854 2021). On the southern margin of the Anguilla Bank, MS5 locally display chaotic reflectors
855 that could indicate slope deposits (Fig. 13B).

856 During the latest Messinian-early Zanclean (SB5) (*ca* 6-4 Ma), the sea level rose by 20
857 m (Miller et al., 2020) but new islands appeared, indicating a regional uplift (Fig. 16G). These
858 new islands, fringed by shallow-water carbonate deposits, emerged from Anguilla to Antigua
859 and shallow-water reefal deposits were emplaced on the Saba Bank. The volcanic islands of the

860 present-day volcanic arc began to emerge by the Pliocene in northwest St Eustatius and
861 southeast St Kitts (e.g., MacDonald et al., 2000). Elsewhere, basin deposits are observed.

862 During the Zanclean-Calabrian (MS6) (4-1 Ma), glacio-eustatic sea level variations
863 could reach 90 m (Miller et al., 2020). The present-day physiography of the northern Lesser
864 Antilles was mostly acquired (Fig. 16H). A regional drowning has however occurred, of greater
865 amplitude than sea level variations, since only small islands remained emerged (St Martin, St
866 Barthélemy, Anguilla, and Antigua). Eastward in the forearc, a drastic subsidence occurred and
867 is likely to be related to margin basal and frontal subduction erosion, which probably accounts
868 for the retreat of the volcanic arc westward (Boucard et al., 2021). Contemporaneously, the
869 volcanic islands of the recent arc emerged, extending from Montserrat to Saba. Discrete
870 synsedimentary faulting is recorded in the southern part of the Kalinago Basin. On the Antigua,
871 Anguilla and Saba Banks, reefal and red algal platforms were emplaced.

872 During the middle and late Pleistocene, several glaciations occurred, coinciding with
873 recurrent up-to-*ca* 120 m- drops in global sea level (e.g., during Marine Isotopic Stages 16a,
874 12a, 10a, 6a, and 2 [at 0.63, 0.44, 0.34, 0.14, and 0.03 Ma, respectively]; Railsback et al., 2015;
875 Miller et al., 2020; Westerhold et al., 2020) (Fig. 16I). Evidence of emersion has been found in
876 carbonate submarine banks, such as Saba Bank, where giant sinkholes, several hundred meters
877 deep, have been recently revealed (van Duyl and Meesters, 2018). These drops had direct
878 consequences on the emerged areas and relationships between the northern Lesser Antilles
879 islands.

880

881 ***6.3. Geodynamic settings since the late Eocene***

882 The strain pattern observed in this study reflects the accommodation of trench bending
883 that followed a plate boundary rearrangement at the northeastern corner of the Caribbean Plate,
884 which originated both from collision between the Bahamas Bank and Greater Arc of the

885 Caribbean with along its northern boundary and a major change in plate kinematics (Boschman
886 et al., 2014; Legendre et al., 2018; Philippon et al., 2020a, b; Boucard et al., 2021). Our
887 palaeogeographical reconstructions (Fig. 16) allow, for the first time, to evidence regional scale
888 vertical motions affecting the whole northern Lesser Antilles. Indeed, we show the emergence
889 of hundreds km- long landmasses along the trench in the arc area and subsequent regional
890 drownings of these lands at the scale of tens Myrs.

891 Following the E-W compression that occurred during the late-middle Eocene (Philippon
892 et al., 2020a), which led to large emerged areas in the northern Lesser Antilles, the tectonic
893 regime changed drastically. Since then, the palaeogeography has been controlled by regional
894 extensional setting leading to alternating episodes of uplift and subsidence. Vertical motions
895 are controlled by two sets of normal faults trending NE-SW and NW-SE, respectively. The
896 Kalinago Basin opened during the late Eocene-early Oligocene and propagated from north to
897 south, between ~34 and ~28 Ma, in intra-arc rift position (MS3). First, this opening was
898 controlled by NW-SE trending normal faults, *i.e.* parallel-to-the-trench. Later on, NW-SE and
899 NE-SW trending regional normal faults affected the northern Lesser Antilles realm (MS3 and
900 MS4) (Jany et al., 1990; Legendre et al., 2018; Boucard et al., 2021; this work). Consistently,
901 NE-SW-trending faults fractured the inner forearc generating deep V-shapes valleys separated
902 by shallow crustal spurs (Boucard et al., 2021). This regional extension in the upper plate
903 possibly resulted from the Bahamas Bank collision and westward drifting, the consecutive
904 margin convex bending and crustal blocks rotations (Mann et al., 2005; Philippon et al., 2020b).
905 This extension might also be consistent with a transient trench rollback (over a short time lapse)
906 during the early stages of extension. Soon after SB3 (late Oligocene erosional surface), the zone
907 of maximum subsidence switched eastward to the forearc, on the eastern margin of the Kalinago
908 Basin where the V-shaped deep basins and Spurs opened during the late Oligocene-early

909 Miocene (Boucard et al., 2021). Volcanism remained active from Antigua to St Barthélemy,
910 and ceased at *ca* 24 Ma in St Barthélemy and St Martin.

911 Between SB4 and SB5 (middle Miocene-early Pliocene) the deformation regime
912 changed. The tectonic activity along the NE-SW faults, which bound the V-shaped basins, has
913 progressively ceased and deep NW-SE faults resulted from an extensive deformation normal to
914 the margin. A significant subsidence affected the forearc and the Kalinago basin. The volcanic
915 arc migrated westward into the arc interior. The margin has likely undergone a long-term frontal
916 erosion compared to the accretionary Central and Southern Lesser Antilles. This frontal erosion,
917 trench landward migration associated with margin extension, fracturing, drastic subsidence and
918 volcanic arc landward retreat testify for enhanced basal erosion of the upper plate (Boucard et
919 al., 2021).

920

921 ***6.4. Faunal dispersals***

922 Our results indicate that prominent uplift events occurred during the late Bartonian-early
923 Priabonian, the Chattian, the Langhian and the early Zanclean in the northern Lesser Antilles.
924 During these intervals, hundred kilometers- long and wide emerged islands extended from
925 Antigua to the Anguilla and Saba Banks (Fig. 16), thus providing more or less continuous
926 terrestrial connections to the Greater Antilles (Puerto Rico and Virgin Islands). Such a
927 connection has been previously proposed but only for the late Eocene (GrANoLA land,
928 Philippon et al., 2020). Whereas it has been unsuspected until now, with this thorough
929 geological and geophysical study of the Northern Lesser Antilles realm, we evidence that the
930 northern part of the Lesser Antilles has been a favourable area that may have allowed the
931 dispersal of terrestrial species between the Greater Antilles and the northern part of South
932 America, not only during the late Eocene but also from the Oligocene to recent times with the
933 episodic formation of emerged archipelagos. Moreover, this potential transit zone identified

934 here, from the Anguilla Bank to the Antigua Bank, can be extended southwards to the
935 Guadeloupe archipelago where, there too, vast island areas have been identified with a similar
936 schedule: at the early Miocene-middle Miocene transition, at the late Miocene-early Pliocene
937 transition and during the Early Pleistocene (De Min, 2014; De Min et al., 2015), aside from
938 Pleistocene sea-level drops controlled by glaciation (Railsback et al., 2015). Thus, the northern
939 Lesser Antilles might have contributed to faunal dispersals at multiple times since the late
940 Eocene. During the late Eocene, the emerged areas in the northern Lesser Antilles were at their
941 maximum and might have been connected to the supposed GAARlandia land bridge, playing a
942 role in the dispersal of South American terrestrial fauna to the Greater Antilles (Iturralde-Vinent
943 and McPhee, 1999). However, later dispersal events have also been evidenced (Fabre et al.,
944 2014; Brace et al., 2015; Courcelle et al., 2019) and they may be supported by the repeated
945 occurrence of more or less important emerged land masses in the northern Lesser Antilles (this
946 work) and possibly in the southern Lesser Antilles, too. The role of the Lesser Antilles in the
947 dispersal of land fauna during the last 40 Myrs must therefore be reassessed, on one hand by
948 searching for a terrestrial fossil record that is currently lacking, and on the other hand by
949 reconstructing the palaeogeography of its southern part between Guadeloupe and Venezuela.

950

951

952 **7. CONCLUSIONS**

953 Our integrated onshore-offshore study of the Cenozoic deposits of the northern part of the
954 Lesser Antilles shows:

- 955 • An isolated reefal platform in Anguilla lasting the whole Aquitanian to Messinian
956 interval (23-*ca* 5.3 Ma); reefal to peri-reefal deposits fringing an island in St Martin and
957 covering the Aquitanian-Zanclean interval (23-3.8 Ma); peri-reefal to slope deposits at
958 Tintamarre with two episodes of mass wasting, which occurred during the late

959 Burdigalian (18-16 Ma) and the early Langhian (15.4-15 Ma), respectively; reefal
960 deposits at Barbuda from the Messinian-Piacenzan(?) (?11.6-?2.5Ma); reefal then deep
961 sea deposits in Antigua spanning the Rupelian-Chattian interval (?33.9-23 Ma).

- 962 • Offshore, we defined seven seismic megasequences (MS) bounded by regional-scale,
963 erosional unconformities. MS1 corresponds to a partly sedimentary Cretaceous to lower
964 Eocene deformed basement; MS2 is a middle-upper Eocene sequence displaying
965 inverted grabens; MS3 deposited during the late Eocene and the early Oligocene; MS4
966 deposited between the late Oligocene and the early Miocene; MS5 deposited between
967 the middle Miocene and the early Pliocene; MS6 and MS7 deposited during the early
968 Pliocene and the Pleistocene.
- 969 • Our palaeogeographical reconstructions highlight uplifts and emergences of hundreds
970 km- long islands during the late Eocene, the late Oligocene, the early Langhian, and the
971 latest Miocene-earliest Pliocene. These uplift events have been interspersed by
972 drowning episodes that occurred during the early Oligocene, the middle Miocene-
973 earliest Pliocene and from the early Pliocene to the present-day. Uplift episodes
974 generated archipelagos with mega-islands and/or neighbouring islands in the Greater
975 Antilles, the Lesser Antilles, and the northern Aves Ridge.
- 976 • A major, first order geodynamical change occurred by the late Eocene (37.8-33.9 Ma):
977 a convergent event occurred during the late middle-early late Eocene (42-37 Ma),
978 related to the collision between the Caribbean Plate and the Bahamas Bank; later, only
979 extension is recorded with alternating uplift and drowning episodes related to an
980 increasing curvature of the trench. The Kalinago Basin opened as an intra-arc basin
981 during the Priabonian-Rupelian (37-28 Ma). The role of the northern Lesser Antilles
982 concerning the dispersal of terrestrial organisms, between the Greater Antilles and

983 northern South America, has to be re-evaluated in the light of our palaeogeographic
984 reconstructions.

985

986 **Acknowledgements**

987 This work was supported by the INSU TelluS-SYSTER grant call 2017, the GAARAnti
988 project (ANR-17-CE31-0009), the GARANTI Cruise (2017) and the ANTITHESIS Cruise
989 (2013). We are indebted to Saba Bank Resources N.V. for the provision of seismic lines of the
990 Saba Bank area. We gratefully thank the captain and crew of *R/V L'Atalante*, as well as the
991 technical staff of Genavir for having successfully completed the acquisition of seismic data and
992 dredge samples during the GARANTI and ANTITHESIS cruises
993 (<https://doi.org/10.17600/17001200>). Multichannel seismic processing was performed with
994 Geovation software of CGG and Seismic Unix. All geophysical data of the ANTITHESIS and
995 GARANTI cruise are available on demand at SISMER (www.ifremer.fr/sismer/). Thin-sections
996 were made by D. Delmas and C. Nevado (Montpellier) and F. Zami (Pointe à Pitre). Paul Mann,
997 an anonymous reviewer and Editor Christopher Fieding are thanked for their constructive
998 reviews.

999

1000

1001

1002

1003

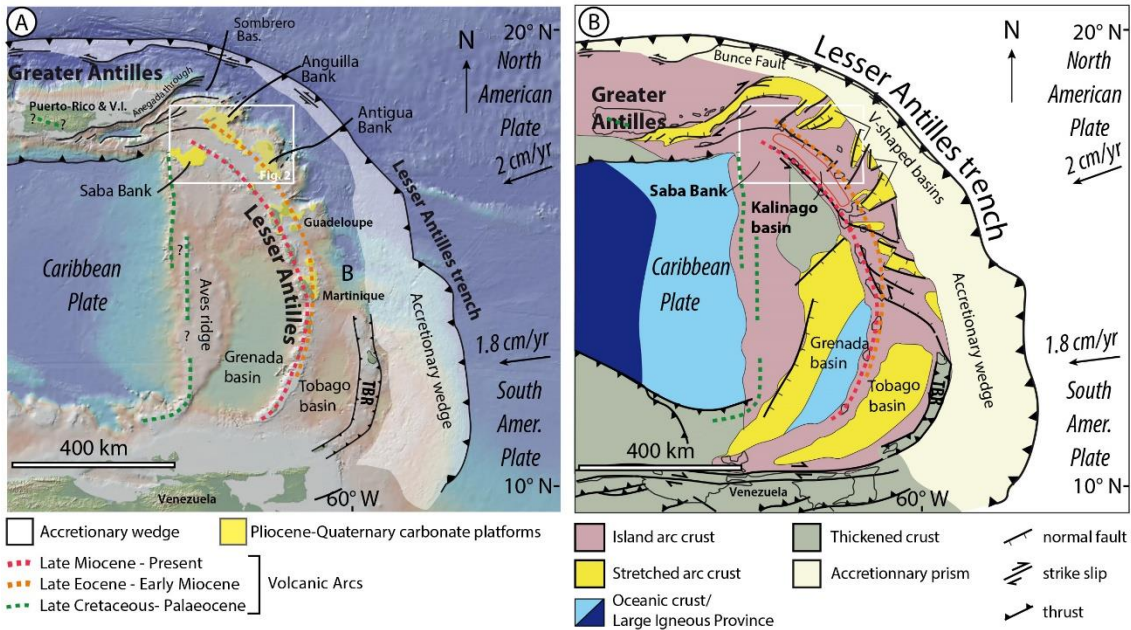
1004

1005

1006

1007

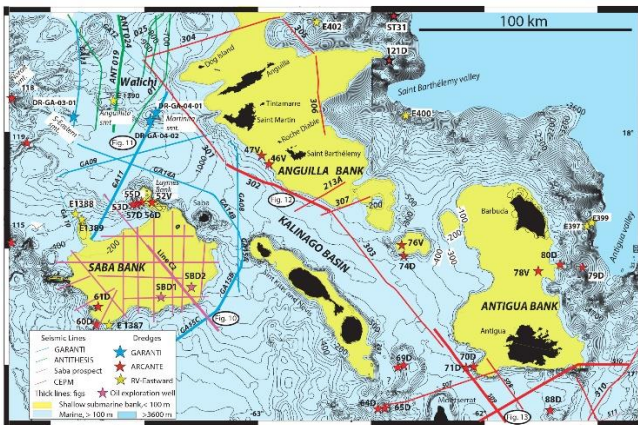
1008 **Figures**



1009 Comée et al., Fig. 1

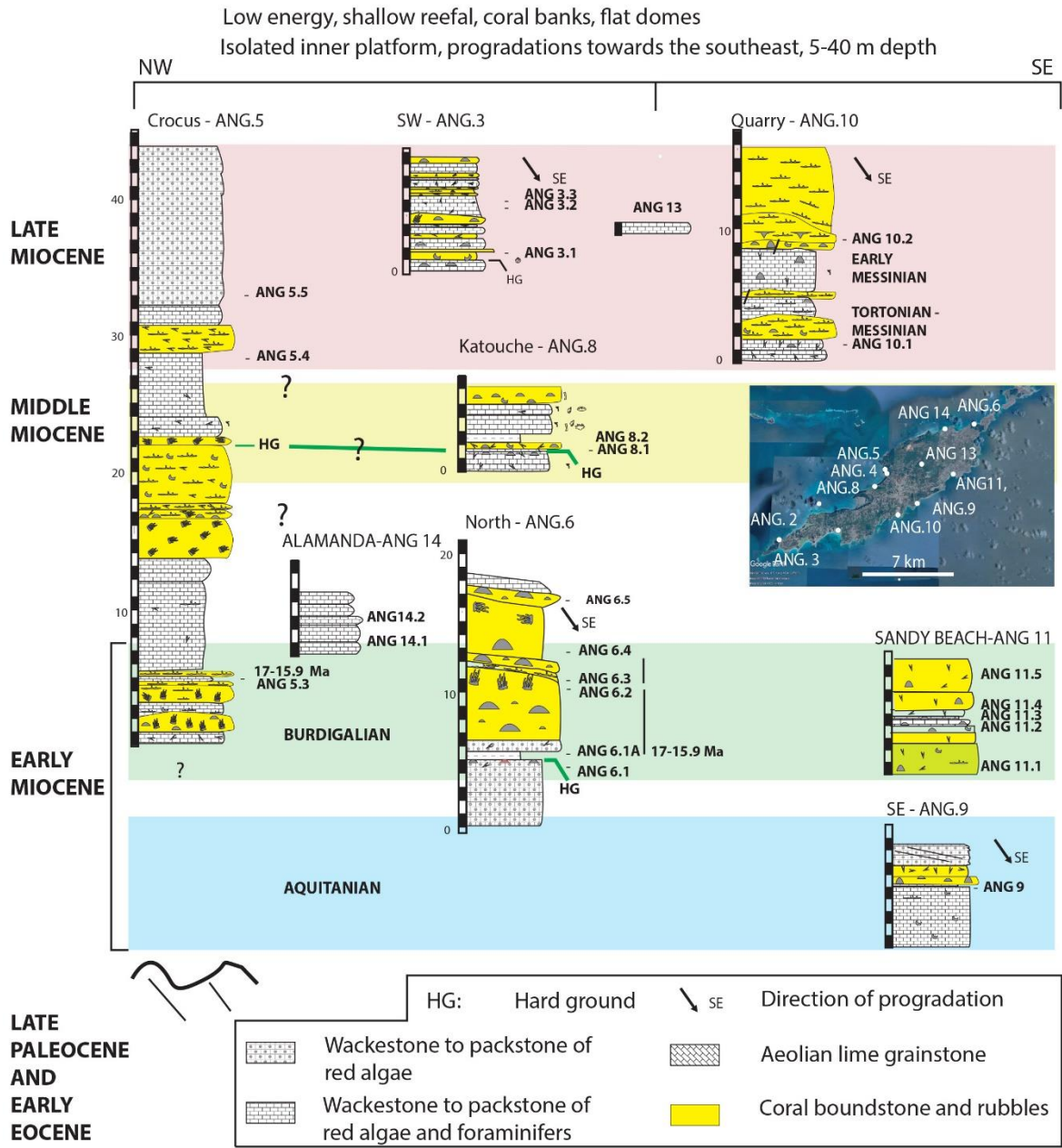
1010 Fig. 1: A: tectonic setting of the Lesser Antilles subduction zone; B: schematic map of the main
 1011 crustal blocks; the main faults are drawn from Jany et al. (1990), Feuillet et al. (2002, 2010),
 1012 Clark et al. (2008), Gomez et al. (2018), Garrocq et al. (2020), Padròn et al. (2020), and
 1013 Boucard et al. (2021). The study area is delineated by the white rectangle. TBR: Tobago
 1014 Barbados Ridge.

1015



1016 Comée et al., Fig. 1

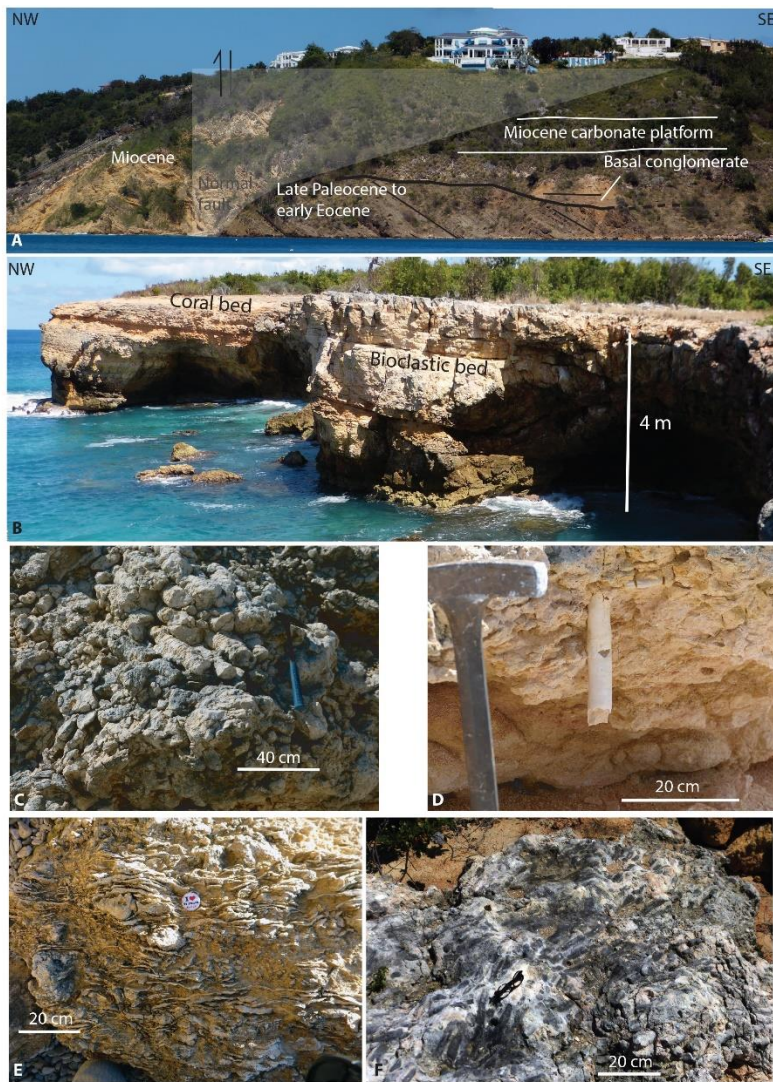
1017 Fig. 2: Location of the studied seismic profiles, dredges and investigated islands of Anguilla
 1018 and Antigua banks. Thick lines correspond to seismic lines of figures 10 to 13.



1020 Cornée et al. Fig. 3

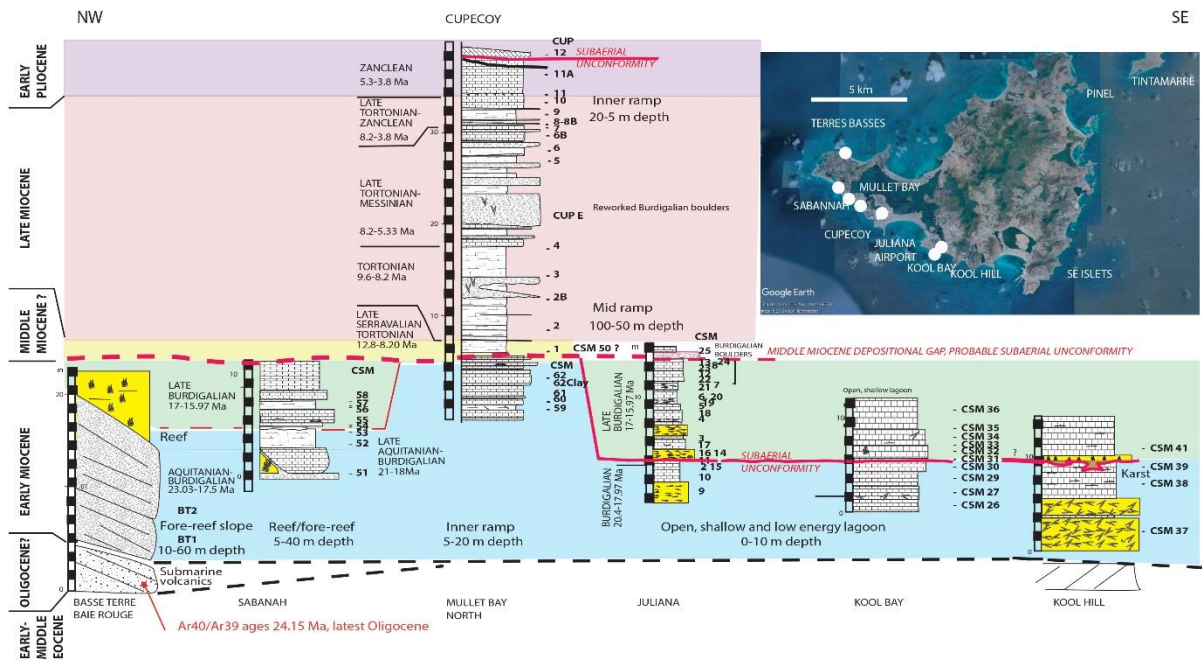
1021 Fig. 3: Correlations of the cross-sections in Anguilla. The location, description and depositional
 1022 settings of the sections, as well as the palaeontological content of the collected samples are
 1023 detailed in Appendix C.

1024



1026 Cornée et al., Fig. 4

1027 Fig. 4: Field view of Anguilla. A: southeastward tilted upper Palaeocene to lower Eocene
 1028 turbidites overlain by sub-horizontal, undated conglomerates then lower Miocene reefal
 1029 carbonates (Crocus Bay); B: typical aspect of the coral and bioclastic banks (locality ANG 3,
 1030 late Miocene; Appendix C); C: detail view of a coral biostromal bed with sub-horizontal thick
 1031 branched *Porites* colonies (locality ANG 6, Burdigalian); D: *Teredo* in life position (locality
 1032 ANG 3, late Miocene); E: sheet-like *Porites* coral colonies with some massive ones (locality
 1033 ANG 10, late Miocene); F: m- high patch reef build-up with branching colonies of
 1034 undertermined genus (locality ANG 3, late Miocene).



1036 Cornée al., Fig. 5

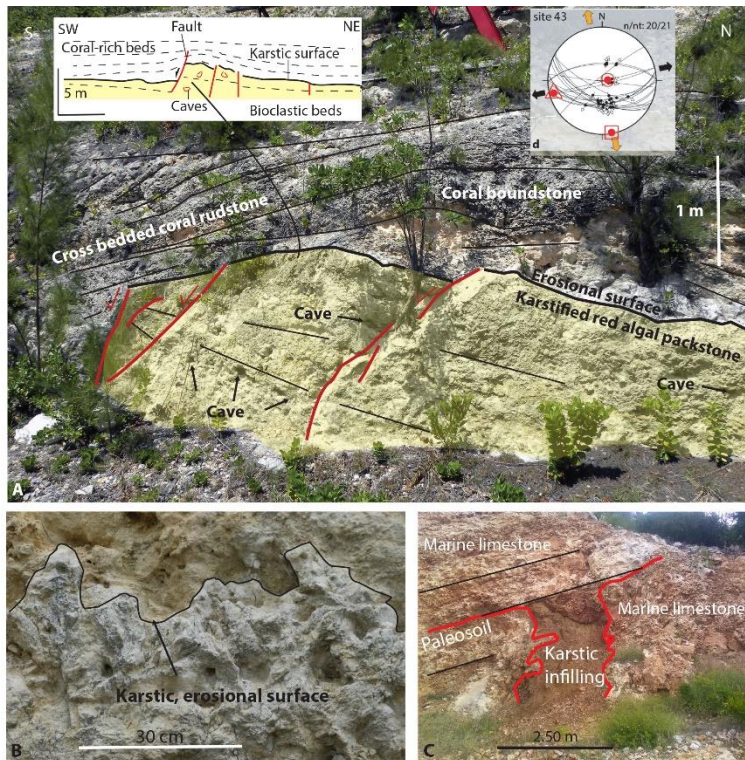
1037 Fig. 5: Correlations in St Martin. The location, description and depositional settings of the
 1038 sections, as well as the palaeontological content of the collected samples, are detailed in
 1039 Appendix D.



1042 Cornée et al., Fig. 6

1043 Fig. 6: Field view of St Martin. A and B: lower Miocene reefal/forereef slope deposits
 1044 composed of coral debris above Oligocene lahars (Terres Basses, Baie Rouge; location in
 1045 Appendix D); C: lagoonal, Burdigalian biostromal coral beds (Juliana airport); D: inner ramp
 1046 patch reefs and associated coral breccias, late Miocene (Cupecoy Bay); E: intra-Zanclean
 1047 erosional surfaces (Cupecoy).

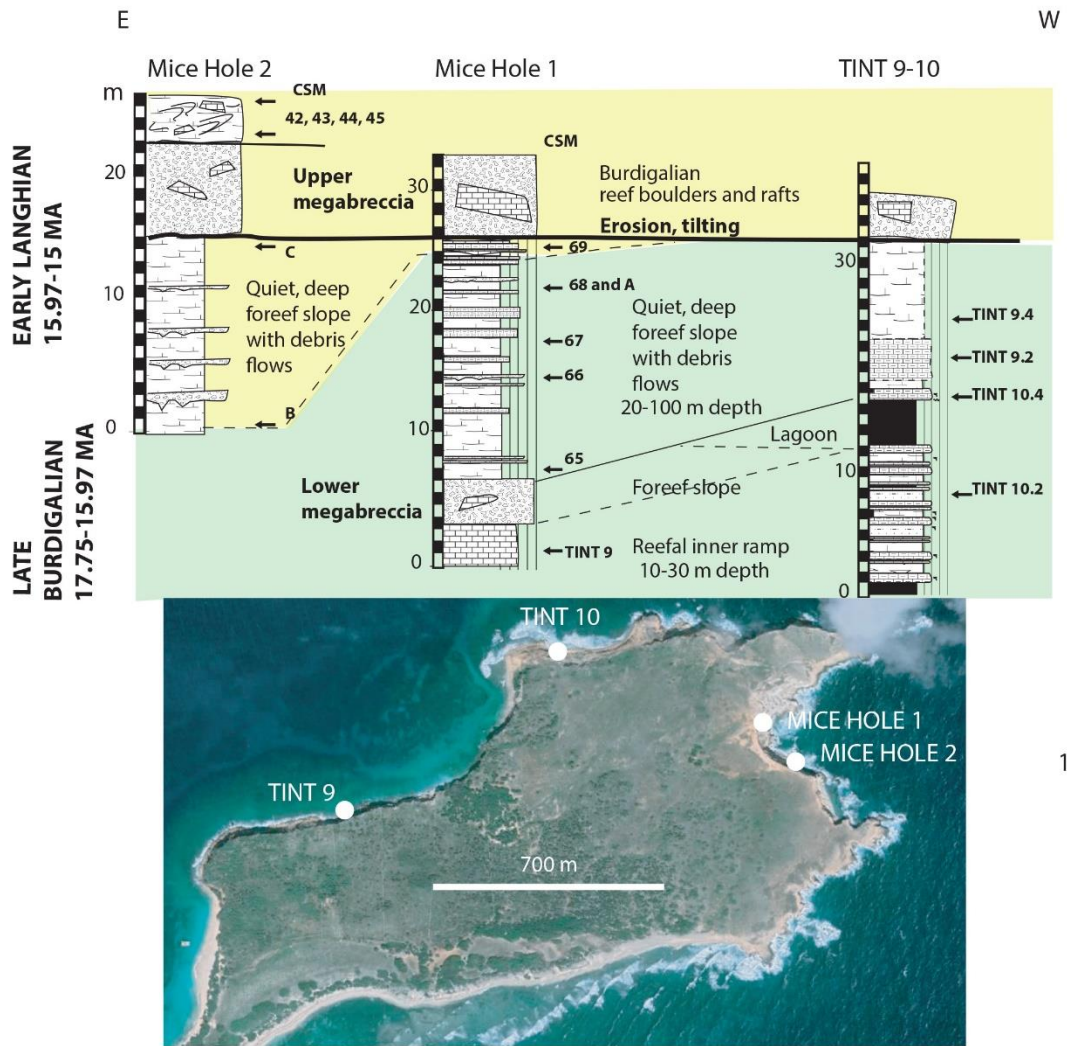
1048



1049 Cornée et al., Fig. 7

1050 Fig. 7: Emergence features in the upper Burdigalian deposits. A: syndimentary normal faults
 1051 in the Burdigalian lagoonal deposits (Juliana airport; stress tensors from Legendre, 2018). The
 1052 horst structure is topped by an emersion surface below which microcaves were found; B:
 1053 detailed view of the emersion surface with karstic gullies sealed by the overlying deposits; C:
 1054 palaeosol and karstic cave infilled with red silty clay within Burdigalian reefal beds; the cave
 1055 is sealed by Burdigalian marine bioclastic limestones (southern side of Kool Hill).

1056



10

1057 Cornée et al. Fig. 8

1058 Fig. 8: Correlations in Tintamarre. The location, description and depositional settings of the
 1059 sections, as well as the palaeontological content of the collected samples are detailed in
 1060 Appendix E.

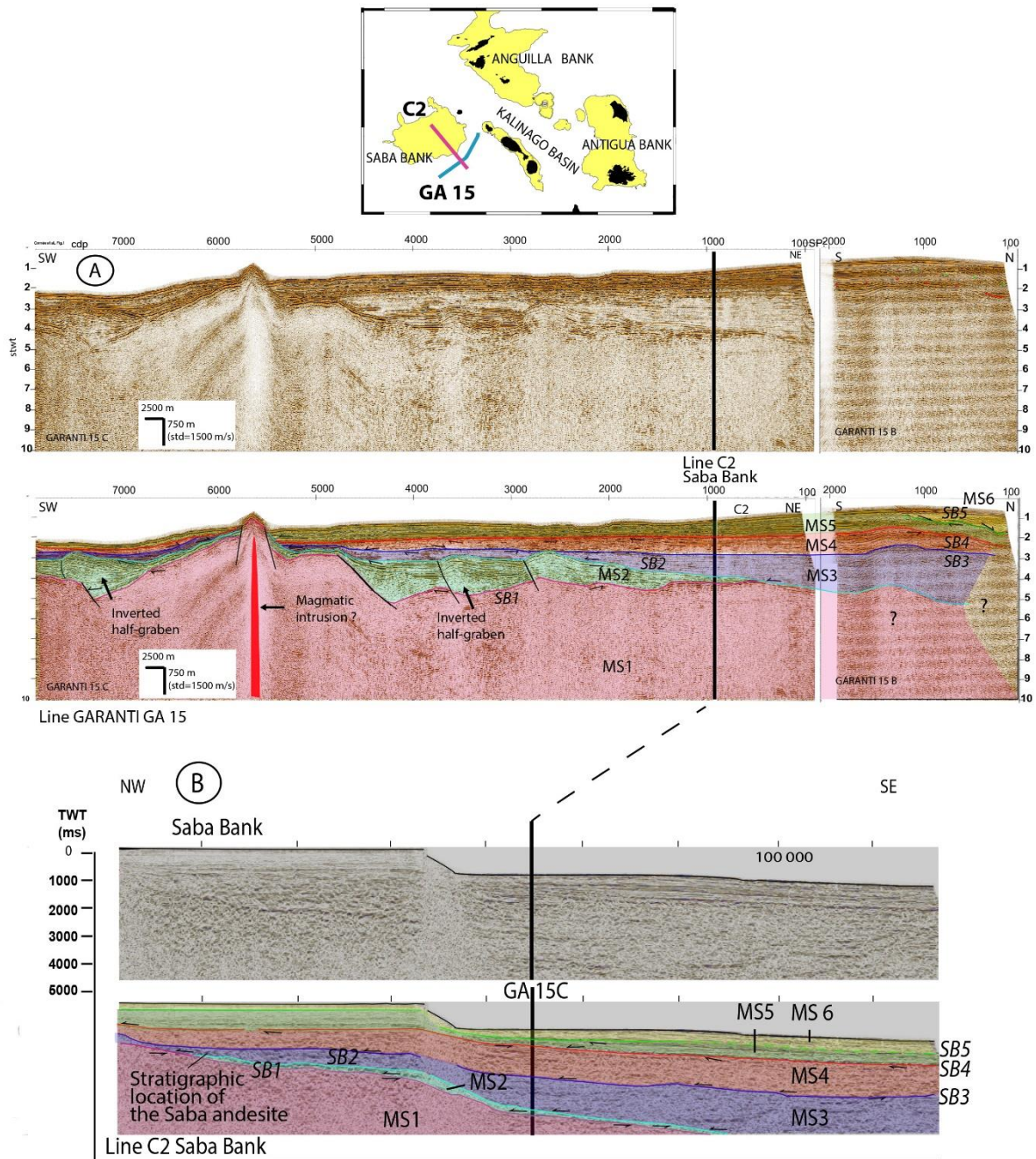
1061

1062



1063 Cornée et al., Fig. 9

1064 Fig. 9: Megabreccias at Tintamarre, locations in Appendix E. A: lower and upper megabreccias
 1065 with early Miocene (20-16 Ma) rafted blocks into bioclastic forereef slope (northern cliff of
 1066 Tintamarre, 200m west from locality TINT 10). In this area, most of the upper Burdigalian and
 1067 lower Langhian deposits have been removed below the upper megabreccia; B: detailed view of
 1068 the middle Miocene (15.4-15 Ma) upper megabreccia consisting of Burdigalian rafted
 1069 limestone beds and dm- to m- wide blocks (Mice Hole 2 locality); C: pink, uppermost part of
 1070 the middle Miocene (15.4-15 Ma) upper megabreccia with m-sized block and large isoclinal
 1071 fold slumps (locality CSM 43).



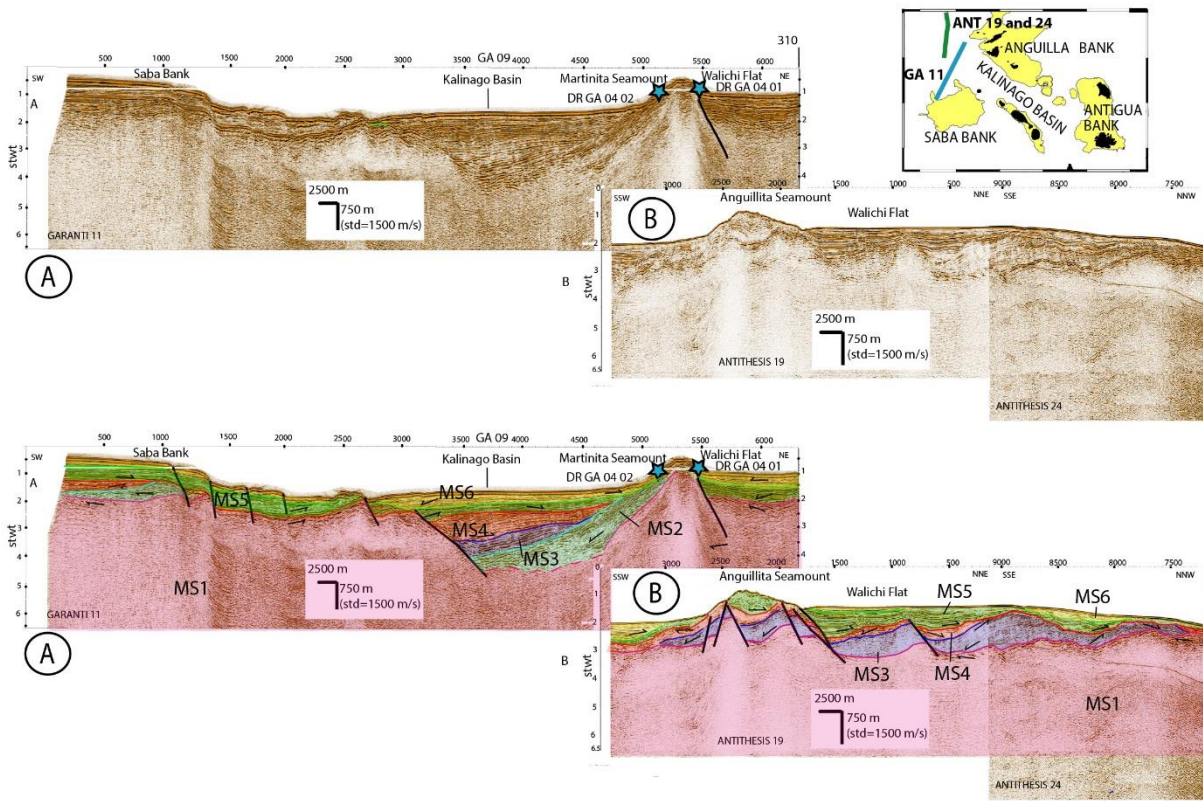
| Units of Church and Allison (2004) | This study North Kalinago | Age of MS | Age of SB |
|---|---------------------------|-------------------------------|--------------------------------------|
| Upper Carbonate Unit | MS6 | Early Pliocene-Pleistocene | SB6 E. Pleistocene |
| | MS5 | Middle Miocene-early Pliocene | SB5 Latest Miocene Early Pliocene |
| Fluvial Deltaic Unit | MS4 | Late Oligocene-early Miocene | SB4 Mid Miocene |
| Andesite then Lower Carbonate and Turbidites Unit | MS3 | Late Eocene-early Oligocene | SB3 Oligocene |
| | MS2 | Eocene | SB2 Late Eocene |
| Cretaceous to Paleocene basement, | MS1 | Cretaceous/Paleocene basement | SB1 Early to middle Eocene? |

1072 Cornée et al. Fig.10

1073 Fig. 10: Reference seismic lines. A: GARANTI GA15 line; B: C2 line (Matchette-Downes,

1074 2007, re-interpreted). MS: megasequence; SB: sequence boundary.

1075



1076

Cornée et al., Fig. 11

1077

Fig.11: A: GARANTI seismic line GA11; B: ANTITHESIS seismic lines 19 and 24. The

1078

Kalinago Rift opened during deposition of MS3 and MS4, which were deposited into syn-

1079

sedimentary half-grabens. MS2 is only preserved in the vicinity of the Martinita Seamount. Some

1080

syn-sedimentary faults were active during deposition of MS3 and M4 only. A part of these fault

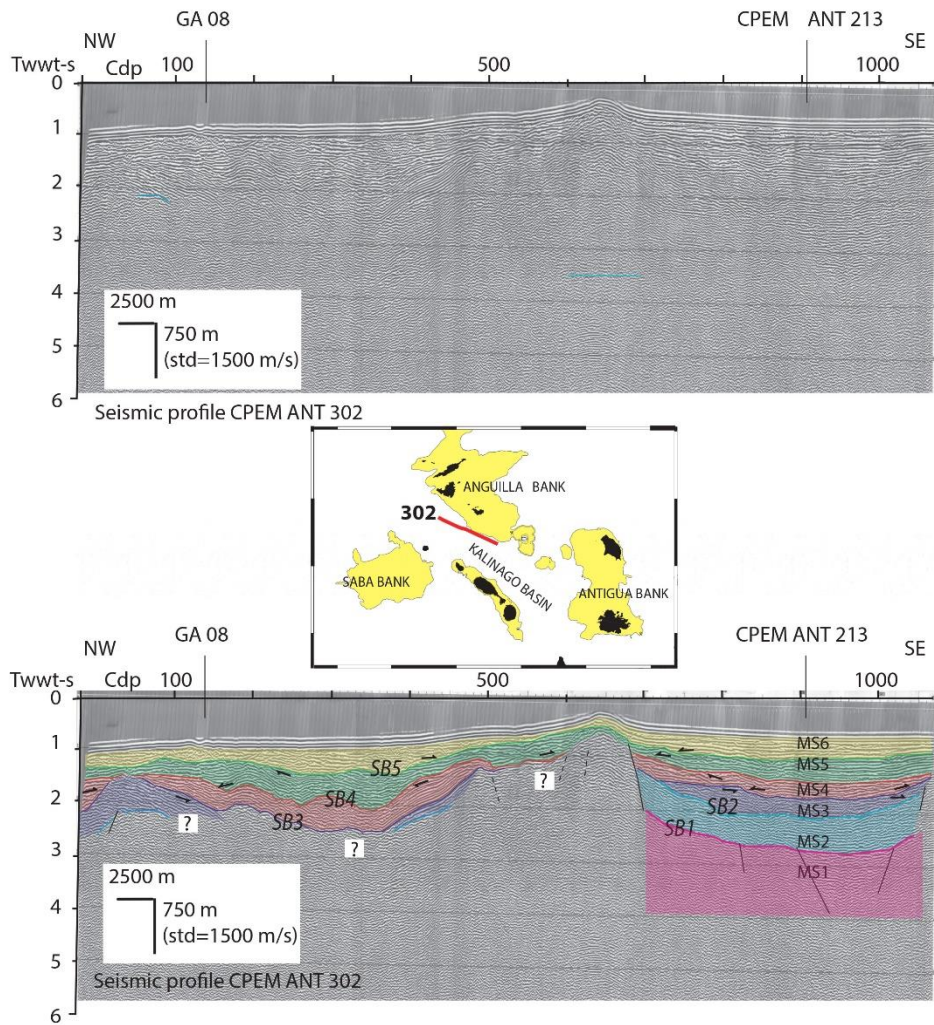
1081

was reactivated later during deposition of MS5 (Anguillita Spur) and others are recent (Saba

1082

bank).

1083

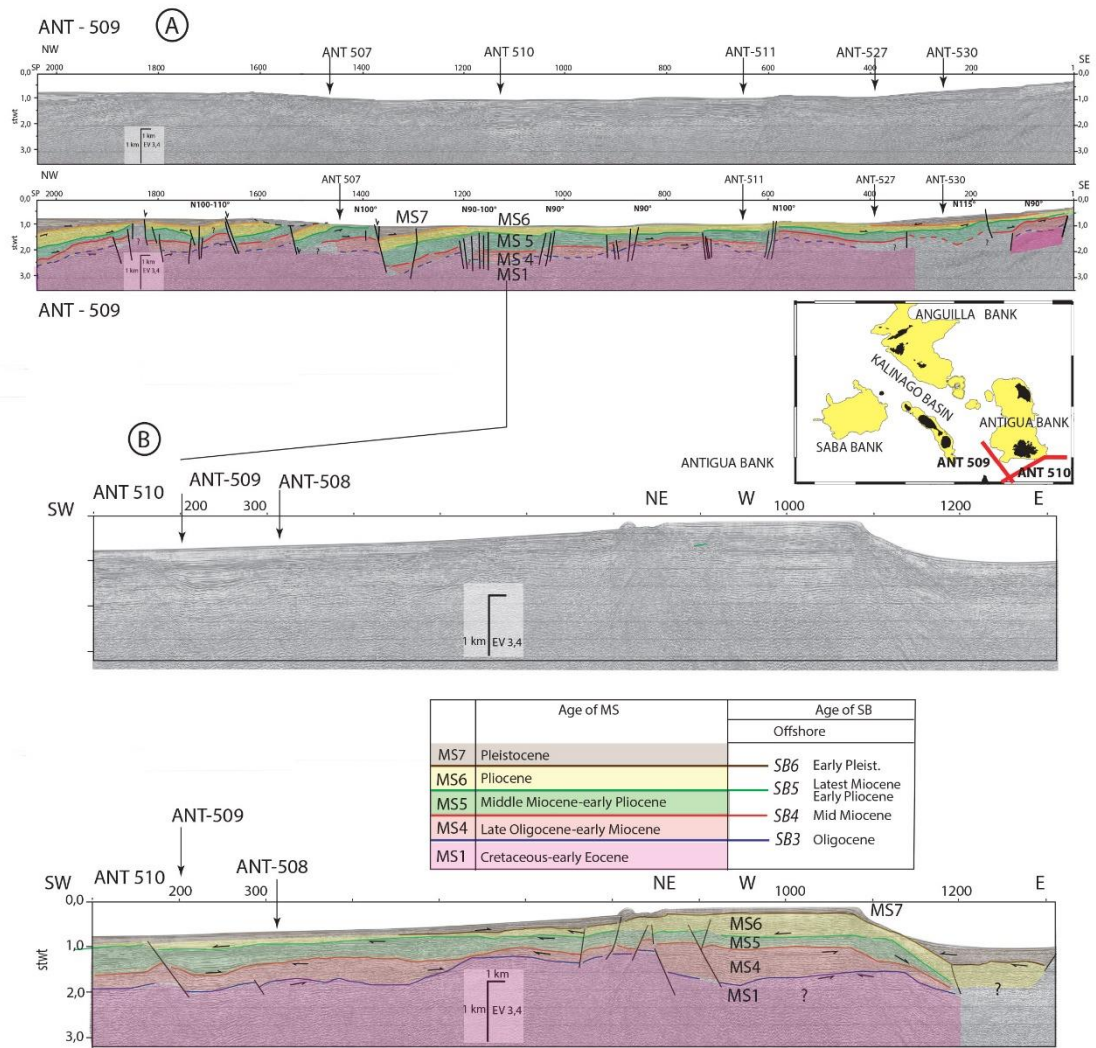


Cornée et al. Fig. 12

1084

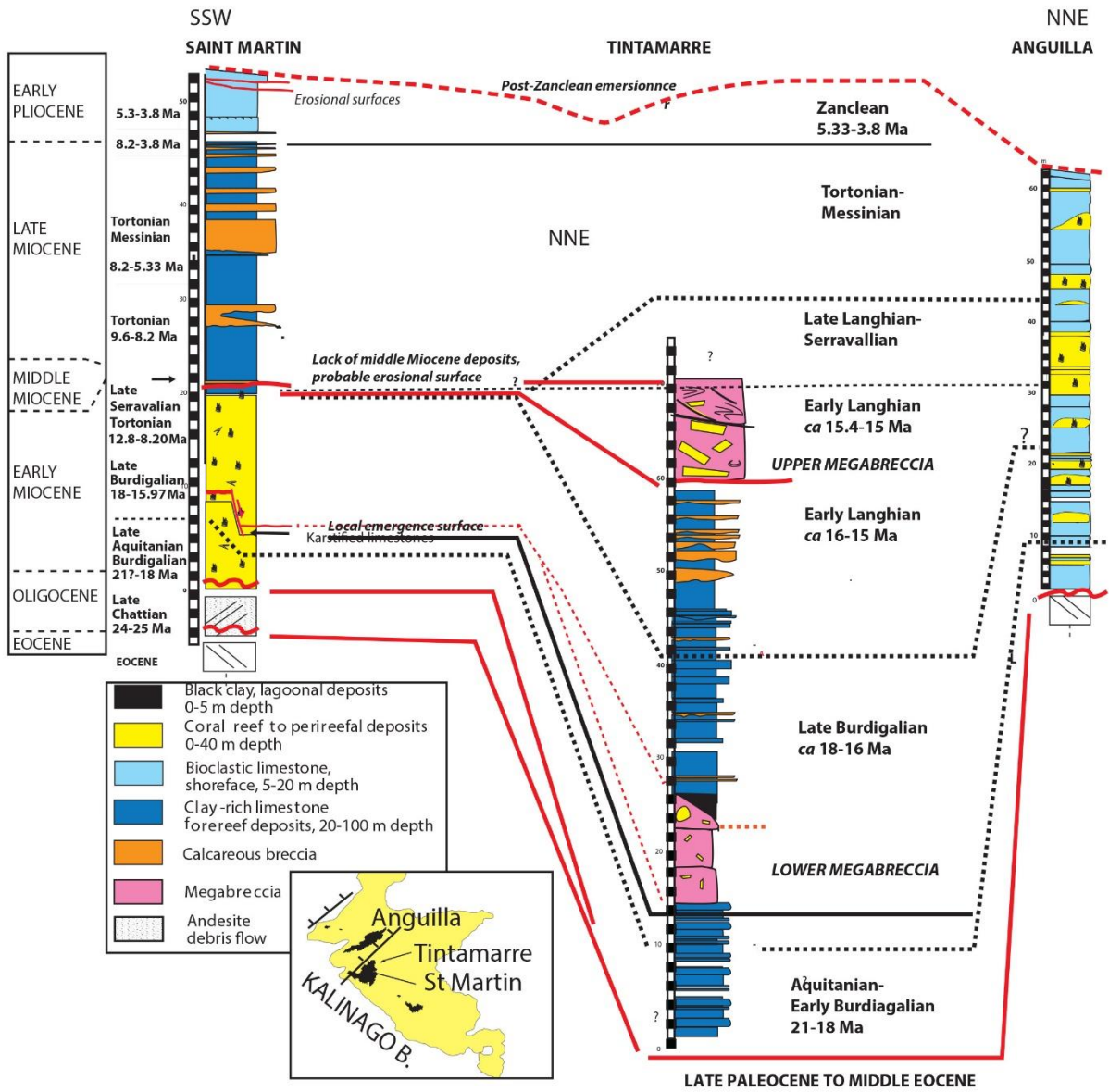
1085 Fig. 12: CPEM seismic line 302. Sequence boundaries display an erosional character. MS2 is
 1086 preserved as a relict patch only to the SE of the seismic profile below SB2. The Kalinago Rift
 1087 opened from MS3 to MS6.

1088



1089 Cornée al., Fig. 14

1090 Fig. 13: A: CPEM line 509; B: CPEM line 510. In the southern part of the Kalinago Basin, MS2
 1091 and MS3 are missing. MS7 can be separated from MS6. The basin opened during deposition of
 1092 MS4 (late Oligocene), later than its northern part (MS3, early Oligocene).



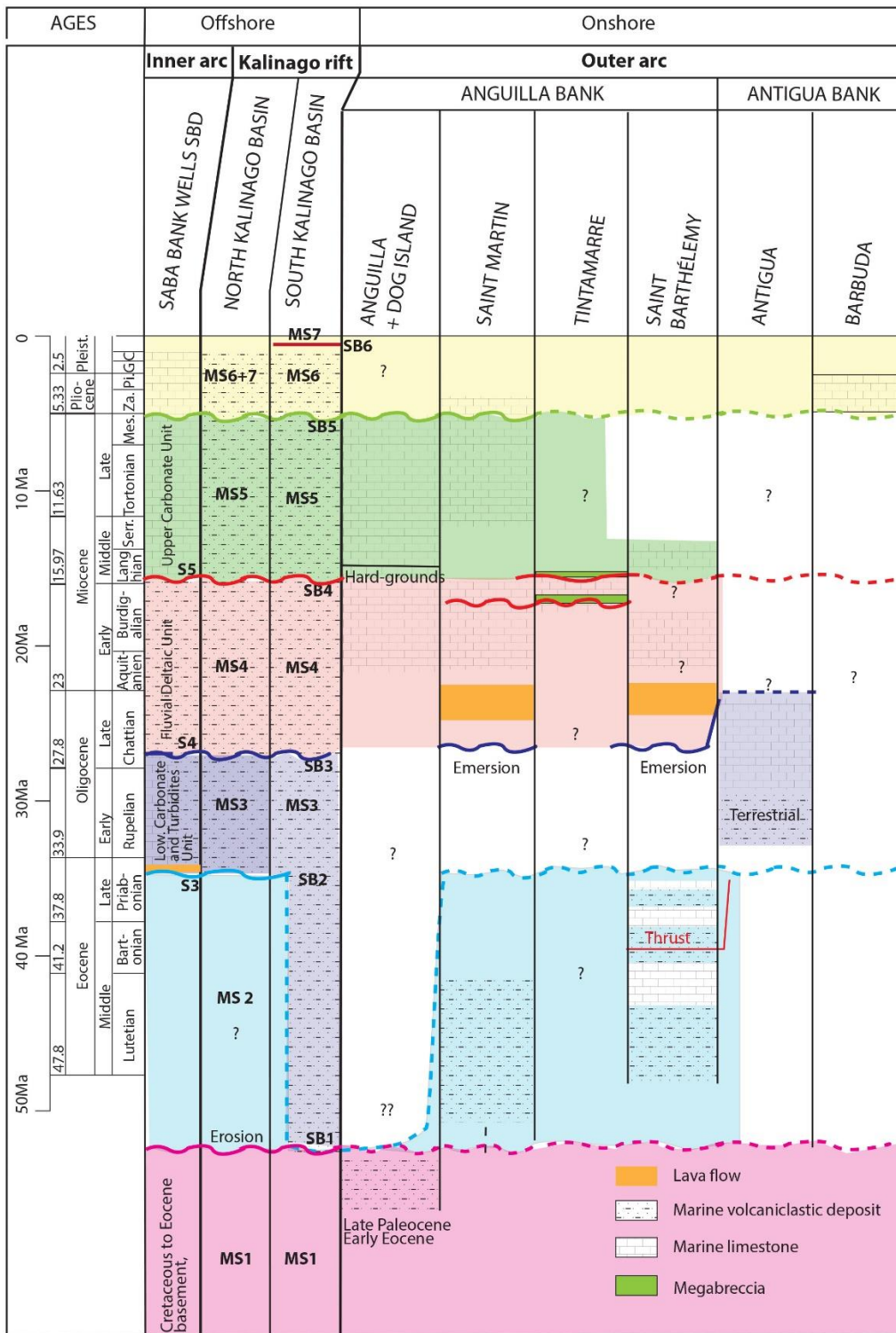
1093

Cornée et al., Fig. 14

1094 Fig. 14: Synthetic Cenozoic lithostratigraphies and correlations of St Martin, Tintamarre and
 1095 Anguilla islands.

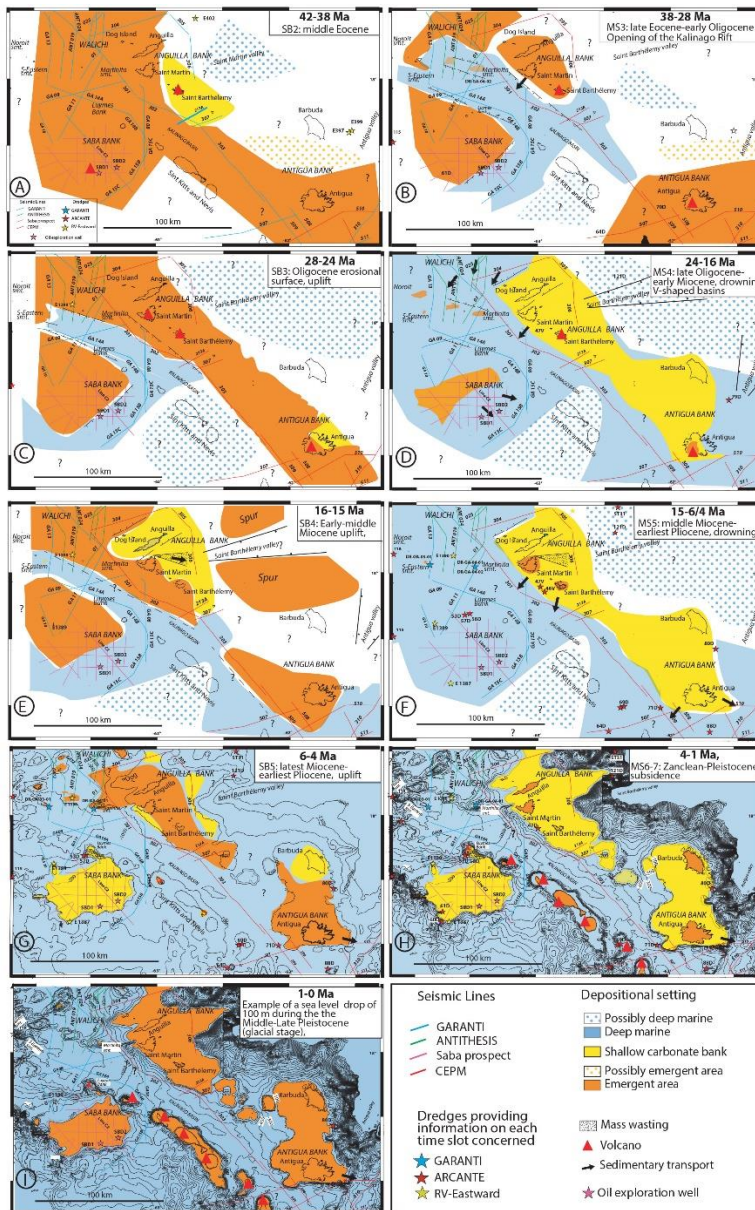
1096

1097



1098 Cornée et al., Fig. 15

1099 15: Onshore-offshore correlations in the northern Lesser Antilles. Onshore, SB2 and SB3 are
 1100 often stacked in a single erosional surface



1101 Cornejo et al., Fig. 16

1102 Fig. 16: Paleogeographic maps of the northern Lesser Antilles, reconstructed from the late
 1103 Eocene to the Middle-Late Pleistocene. A: end of late Eocene compression; B: opening
 1104 of the Kalinago Basin; C: propagation of the Kalinago Basin; D: late Oligocene-early
 1105 Miocene drowning; E: opening of the V-shaped basins and uplift (Boucard et al., 2021);
 1106 F: middle Miocene-earliest Pliocene drowning; G: latest Miocene-earliest Pliocene
 1107 uplift; H: Zanclean-Calabrian drowning; I: example of emerged areas during middle-
 1108 late Pleistocene glacial maxima (considering 100 m sea level drops). **Supplementary**
 1109 **data**

1110

1111 Appendix A: Microphotographs of stratigraphically significant calcareous nannofossil taxa
1112 from the samples collected in the northern Lesser Antilles. Appendix B: Microphotographs of
1113 stratigraphically significant foraminiferal taxa from the samples collected in the northern Lesser
1114 Antilles.

1115

1116 Appendix C: Lithostratigraphical successions of Anguilla with depositional settings and
1117 microfossil content.

1118

1119 Appendix D: Lithostratigraphical successions of St Martin with depositional settings and
1120 microfossil content.

1121

1122 Appendix E: Lithostratigraphical successions of Tintamarre with depositional settings and
1123 microfossil content.

1124

1125 Appendix F: Lithostratigraphical succession of the Highland Fm. of Barbuda with depositional
1126 settings and microfossil content.

1127

1128 Appendix G: Lithostratigraphical successions of St Barthélemy and Antigua with depositional
1129 settings and microfossil content.

1130

1131 Appendix H: Dredged samples in the northern Lesser Antilles; locations Fig. 2.

1132

1133 Appendix I: Samples dredged during the cruise GARANTI: facies, depositional settings and
1134 microfossil contents.

1135
1136 Appendix J: Seismic lines CPEM 213 (Bouysse et al., 1994, re-interpreted) and GARANTI
1137 GA08 and 09.

1138
1139 Appendix K: Radiometric dating of a lava in St Martin, Terres Basses.

1140

1141 **References**

1142 Ali JR., 2012 Colonizing the Caribbean: is the GAARLandia land-bridge hypothesis gaining a
1143 foothold? *J. Biogeogr.* 39, 431–433. [doi:10.1111/j.1365-2699.2011.02674.x](https://doi.org/10.1111/j.1365-2699.2011.02674.x)

1144
1145
1146 Andréieff P., Bouysse P. and Westercamp D., 1980. Reconnaissance géologique de l'arc
1147 insulaire des Petites Antilles. Résultats d'une campagne à la mer de prélèvements de roches
1148 entre Sainte Lucie et Anguilla. Rapport Bur. Géol. Min., Orléans (F), 80 SGN 086 MAR, 70
1149 pp.

1150
1151 Andréieff P., Bouysse P. and Westercamp D., 1987. Géologie de l'arc insulaire des Petites
1152 Antilles, et évolution géodynamique de l'ESTCaraiïbe, Thèse de Doctorat d'état, Université de
1153 Bordeaux I.

1154
1155 Andréieff P., Baubron J.C. and Westercamp D., 1988a. Histoire géologique de la Martinique
1156 (Petites Antilles): biostratigraphie (foraminifères), radiochronologie (potassium–argon),
1157 évolution volcano-structurale. *Géol. Fr.*, 2-3, 39-70.

1158
1159 Andréieff P., Westercamp D., Garrabé F. and Bonneton J.R., 1988b. Stratigraphie de l'île de
1160 Saint-Martin. *Géol. Fr.*, 2-3, 71-88.

1161
1162 Boschman L. M., van Hinsbergen D. J. J., Torsvik T. H., Spakman, W. and Pindell, J. L.,
1163 2014. Kinematic reconstruction of the Caribbean region since the Early Jurassic. *Earth-Sci.*
1164 *Rev.*, 138, 102-136.

1165
1166 Boucard M., Lebrun J.-F., Marcaillou B., Laurencin M., Klingelhoefer, F., Laigle, M.,
1167 Lallemand, S., Schenini L., Graindorge D., Cornée J.-J., Münch, P., Philippon M., and the
1168 ANTITHESIS 1, 3 Teams, 2021 (in press). Paleogene V-shaped basins and Neogene
1169 subsidence of the Northern Lesser Antilles forearc. *Tectonics*.

1170 <https://doi.org/10.1029/2020TC006524>

1171
1172 Boudagher-Fadel M. K., 2008. Evolution and significance of larger benthic foraminifera. In :
1173 Developments in Paleontology and stratigraphy 21 (ed. P. B. Wignall), 540 pp., Amsterdam,
1174 Elsevier.

1175
1176 Boudagher-Fadel M. K., 2015. Biostratigraphic and Geological Significance of Planktonic
1177 Foraminifera (Updated 2nd Edition). London, UCL Press, 298 pp.
1178 [doi:10.14324/111.9781910634257](https://doi.org/10.14324/111.9781910634257)

1179
1180 Boudagher-Fadel M.K., 2018. Revised Diagnostic First and Last Occurrences of Mesozoic
1181 and Cenozoic Planktonic Foraminifera. UCL Office of the Vice-Provost Research,
1182 Professional Papers Series, 2, 1-5. <http://www.es.ucl.ac.uk/people/fadel/home-mkf.htm>
1183
1184 Bouysse P. and Guennoc P., 1983. Données sur la structure de l'arc insulaire des Petites
1185 Antilles entre St Lucie et Anguilla. *Mar. Geol.* 53, 131– 166.
1186
1187 Bouysse P. and Mascle A., 1994. Sedimentary Basins and Petroleum Plays Around the French
1188 Antilles. In: Mascle A. (eds) Hydrocarbon and Petroleum Geology of France. Special
1189 Publication of the European Association of Petroleum Geoscientists, 4. Springer.
1190 https://doi.org/10.1007/978-3-642-78849-9_3
1191
1192 Bouysse P., Andréïeff P., Richard M., Baudron J.C., Mascle A., Maury R. and Westercamp,
1193 D., 1985a. Aves swell and northern Lesser Antilles Ridge: Rock-dredging results from
1194 ARCANTE 3 cruise. In: A. Mascle (Ed.), Caribbean geodynamics, Technip, Paris 65-76.
1195
1196 Bouysse P., Baudron J.C., Richard M., Maury R. and Andréïeff P., 1985b. Evolution de la
1197 terminaison nord de l'arc interne des Petites Antilles au Plio-Quaternaire. *Bull.Soc.géol. Fr.*, I,
1198 181–188. <https://doi.org/10.2113/gssgfbull.i.2.181>
1199
1200 Brace S., Turvey S. T., Weksler M., Hoogland M. L. P. and Barnes I., 2015. Unexpected
1201 evolutionary diversity in a recently extinct Caribbean mammal radiation. *Proc. Roy.Soc.*
1202 *London*, B, 282, 20142371.
1203
1204 Brasier M. D. and Mather J.D., 1975. The stratigraphy of Barbuda, West Indies. *Geol. Mag.*,
1205 112, 271-282.
1206
1207 Brasier M.D. and Donahue J., 1985. Barbuda-An emerging reef and lagoon complex on the
1208 edge of the Lesser Antilles island arc. *J. geol. Soc. London*, 142, 1101-1117.
1209
1210 Briden J. C., Rex D. C., Faller A. M. and Tomblin J. F., 1979. K-Ar geochronology and
1211 palaeomagnetism of volcanic rocks in the Lesser Antilles island arc. *Philos. Trans. Royal Soc.*
1212 *A: Mathematical, Physical and Engineering Sciences*, 291, 485–528.
1213 doi.org/10.1098/rsta.1979.0040
1214
1215 Budd A.F., Johnson K.G. and Edwards J.C., 2005. Caribbean reef coral diversity during the early
1216 to middle Miocene: an example from the Anguilla Formation. *Coral reefs*, 14, 109-117.
1217
1218 Calais E., Symithe S., de Lépinay B. M. and Prépetit C., 2016. Plate boundary segmentation
1219 in the northeastern Caribbean from geodetic measurements and Neogene geological
1220 observations. *C. R. Geoscience*, 348, 42-51.
1221
1222 Carey S., Sparks R. S. J., Tucker M. E., Li T., Robinson L., Watt S. F. L., ... and Ballard R.
1223 D., 2020. The polygenetic Kahouanne Seamounts in the northern Lesser Antilles island arc:
1224 evidence for large-scale volcanic island subsidence. *Marine Geology*, 419,
1225 <https://doi.org/10.1016/j.margeo.2019.106046>.
1226
1227 Cattuneanu O., 2006. Principles of sequence stratigraphy. Elsevier, 369 pp.
1228

1229 Chaytor J. D. and ten Brink U. S., 2015. Event sedimentation in low-latitude deep-water
1230 carbonate basins, Anegada Passage, northeast Caribbean. *Basin Res.*, 27, 310–335.
1231 [doi:10.1111/bre.12076](https://doi.org/10.1111/bre.12076).

1232
1233 Christman R. A., 1953. Geology of St Bartholomew, St Martin, and Anguilla, Lesser Antilles.
1234 *Geol. Soc. Amer., Bull.*, 64, 65–96. [https://doi.org/10.1130/0016-
1235 7606\(1953\)64%5B85:GOSBSM%5D2.0.CO;2](https://doi.org/10.1130/0016-7606(1953)64%5B85:GOSBSM%5D2.0.CO;2)
1236

1237 Church R. E. and Allison K. R., 2004. The Petroleum Potential of the Saba Bank Area, Netherlands
1238 Antilles. Search and
1239 Discovery Article # 10076. Posted December 20, 2004

1240 Clark, S.A., Sobiesiak, M., Zelt, C.A., Magnani, M.B., Miller, M.S., Bezada, M.J.,
1241 Levander, A., 2008. Identification and tectonic implications of a tear in the South American
1242 plate at the southern end of the Lesser Antilles. *Geochemistry, Geophysics, Geosystems*, 9,
1243 Q11004. [doi:10.1029/2008GC002084](https://doi.org/10.1029/2008GC002084).

1244
1245 Cornée J.-J., Léticée J.-L., Münch P., Quillévééré F., Lebrun J.-F., Moissette P., Braga J.C.,
1246 Melinte- Dobrinescu M., De Min L., Oudet J., Randrianasolo A., 2012. Sedimentology,
1247 paleoenvironments and biostratigraphy of the Pliocene-Pleistocene carbonate platform of
1248 Grande- Terre (Guadeloupe, lesser Antilles fore-arc). *Sedimentology*, 59, 1426-1451.
1249

1250 Cornée J.-J., BouDagher-Fadel M., Philippon M., Léticée J.-L., Legendre L., Maincent G.,
1251 Lebrun J.-F., and Münch P., 2020 Paleogene carbonate systems of Saint Barthélemy, Lesser
1252 Antilles: stratigraphy and general organisation. *Newsl. Stratigr.* [doi:10.1127/nos/2020/0587](https://doi.org/10.1127/nos/2020/0587).
1253

1254 Courcelle M., Tilak M.-K., Leite Y. L. R., Douzery E. J. P. and Fabre, P.-H., 2019. Digging
1255 for the spiny rat and hutia phylogeny using a gene capture approach, with the description of a
1256 new mammal subfamily. *Mol. Phylog. Evol.*, 136, 241-253.
1257

1258 Coussens M.F. *et al.*, 2012. Synthesis: stratigraphy and age control for IODP Sites U1394,
1259 U1395, and U1396 offshore Montserrat in the Lesser Antilles. *In: Le Friant, A., Ishizuka, O.,*
1260 *Stroncik, N.A., and the Expedition 340 Scientists. Proc. IODP 340.*
1261 [doi:10.2204/iodp.proc.340.204.2016](https://doi.org/10.2204/iodp.proc.340.204.2016).
1262

1263 Dagain J., Andréieff P., Westercamp D., Bouysse P. and Garrabé F., 1989. Carte géologique de
1264 France (1:50000), feuille Saint Martin. Bureau de Recherches Géologiques et Minières, Orléans
1265 (Fr).
1266

1267 Dávalos L. M., 2004. Phylogeny and biogeography of Caribbean mammals. *Biol. J. Linnean*
1268 *Soc.*, 81, 373-394.
1269

1270 Dailey S.K., Clift P.D., Kulhanek D.K *et al.*, 2019. Large-scale mass wasting on the Miocene
1271 continental margin of western India. *Geol. Soc. Amer. Bull.*, 132, 85-112.
1272 doi.org/10.1130/B35158.1
1273

1274 Daly T.E. (1995) The Petroleum Potential of the Netherlands Antilles. *In: Miller R.L., Escalante*
1275 *G., Reinemund J.A., Bergin M.J. (eds), Energy and Mineral Potential of the Central American-*
1276 *Caribbean Region. Circum-Pacific Council for Energy and Mineral Resources Earth Science*
1277 *Series, 16, Springer.* https://doi.org/10.1007/978-3-642-79476-6_14

1278 Defand M.J., Sherman S., Maury R.C., Bellon H. de Boer J., Davidson J. and Kepezhinskas
1279 P., 2001. The geology, petrology, and petrogenesis of Saba Island, Lesser Antilles. *J. Volc.*
1280 *Geoth. Res.*, 107, 87-111.
1281
1282 Delsuc F., Kuch M., Gibb G. C., Karpinski E., Hackenberger D., Szpak P., Martinez J. G.,
1283 Mead J. I., McDonald H. G., MacPhee R. D. E. Billet, G., Hautier L. and Poinar H. N., 2019.
1284 Ancient mitogenomes reveal the evolutionary history and biogeography of sloths. *Current*
1285 *Biology*, 29, 1-12.
1286
1287 De Min L., 2014. Sismo-stratigraphie multi-échelle d'un bassin avant-arc: Architecture du
1288 bassin de Marie-Galante, Petites Antilles. Sciences de la Terre. *PhD Thesis*, Université des
1289 Antilles et de la Guyane (UAG), Pointe à Pitre, Guadeloupe, F. [https://hal.archives-](https://hal.archives-ouvertes.fr/tel-03144281)
1290 [ouvertes.fr/tel-03144281](https://hal.archives-ouvertes.fr/tel-03144281)
1291
1292 De Min L., Lebrun J. F., Cornée J. J., Münch P., Léticée J. L., Quillévére, F., et al., 2015.
1293 Tectonic and sedimentary architecture of the Karukéra spur: A record of the Lesser Antilles
1294 fore-arc deformations since the Neogene. *Marine Geology*, 363, 15–37.
1295 <https://doi.org/10.1016/j.margeo.2015.02.007>
1296
1297 Donovan S. K., Jackson T. A., Harper D. A., Portell, R. W. and Renema W., 2014. The upper
1298 Oligocene of Antigua: the volcanic to limestone transition in a limestone Caribbean. *Geology*
1299 *Today*, 30, 151-158.
1300
1301 Fabre P.-H., Vilstrup J. T., Raghavan M., Der Sarkissian C., Willerslev E., Douzery E. J. P.
1302 and Orlando, L., 2014. Rodents of the Caribbean: origin and diversification of hutias
1303 unravelled by next-generation museomics. *Biol. Lett.*, 10, 20140266.
1304
1305 Favier A., Lardeaux J.-M., Legendre L., Verati C., Philippon M., Corsini M., Münch P. and
1306 Ventalon S., 2019. Tectono-metamorphic evolution of shallow crustal levels within active
1307 volcanic arcs. Insights from the exhumed Basal Complex of Basse-Terre (Guadeloupe, French
1308 West Indies). *BSGF - Earth Sci. Bull.*, 190, 10. <https://doi.org/10.1051/bsgf/2019011>
1309
1310 Feuillet, N., Manighetti, I., Tapponnier, P., Jacques, E., 2002. Arc parallel extension and
1311 localization of volcanic complexes in Guadeloupe, Lesser Antilles. *J. Geophys. Res.: Solid*
1312 *Earth*, 107 ETG 3-1–ETG 3-29.
1313
1314 Feuillet N., Leclerc F., Tapponnier P., Beauducel F., Boudon G., Le Friant A., Deplus C.,
1315 Lebrun J.-F., Nercessian A., Saurel J.-M. and Clément V., 2010. Active faulting induced by
1316 slip partitioning in Montserrat and link with volcanic activity: New insights from the 2009
1317 GWADASEIS marine cruise data. *Geoph. Res. Letters*, 37, L00E15. [doi:10.1029/2010GL042556](https://doi.org/10.1029/2010GL042556),
1318
1319 Feuillet N., Beauducel F. and Tapponnier P., 2011. Tectonic context of moderate to large
1320 historical earthquakes in the Lesser Antilles and mechanical coupling with volcanoes. *J.*
1321 *Geophys. Res.: Solid Earth* 116(B10).
1322
1323 Fox P. J., Schreiber E. and Heezen B. C., 1971. The geology of the Caribbean crust: Tertiary
1324 sediments, granitic and basic rocks from the Aves Ridge. *Tectonophysics*, 12, 89–109.

1325 Frost S.H. and Weiss M.P., 1979. Patch reef communities and succession in the Oligocene of
1326 Antigua, West Indies. *Geol. Soc. Amer. Bull.*, 90, 1094-1141.
1327

1328 Garrocq C., Lallemand S., Marcaillou B., Lebrun J.-F., Padron C., Klingelhofer F., Laigle
1329 M., Munch P., Gay A., Shenini L., Beslier M.-O., Cornée J.-J., Mercier De Lepinay B.,
1330 Quillevère F. and Boudagher-Fadel M., 2020. Genetic relations between the Aves Ridge and
1331 the Grenada back-arc basin, East Caribbean Sea. *J. Geophys. Res. Solid Earth*, 126,
1332 e2020JB020466. <https://doi.org/10.1029/2020JB020466>
1333

1334 Gomez S., Bird D. and Mann P., 2018. Deep crustal structure and tectonic origin of the Tobago-
1335 Barbados ridge. *Interpretation*, 6 (2): T471–T484. <https://doi.org/10.1190/INT-2016-0176.1>
1336

1337 Gradstein F. M., Ogg J. G., Schmitz M. D., Ogg G. M., 2012. The Geologic Time Scale 2012.
1338 Elsevier, 1- 144.

1339 Hastie A.R., Cox S. and Kerr A.C., 2021. Northeast- or southwest-dipping subduction in the
1340 Cretaceous Caribbean gateway? *Lithos*. <https://doi.org/10.1016/j.lithos.2021.105998>
1341

1342 Hedges S. B., 1996. Historical biogeography of West Indian vertebrates. *Ann. Rev. Ecol.*
1343 *System.*, 27, 163-196.
1344

1345 Hedges S.B., 2001. Caribbean biogeography: an outline. In: Biogeography of the West Indies:
1346 patterns and perspectives (eds CA Woods, FE Sergile), CRC Press, Boca Raton, FL ,15–33.
1347

1348 Hedges S.B., 2006. Palaeogeography of the Antilles and origin of the West Indian terrestrial
1349 vertebrates. *Annals of the Missouri Botanical Garden*, 93, 231-244.
1350

1351 Hedges S.B., Hass C.A., Maxson L.R., 1992. Caribbean biogeography: molecular evidence
1352 for dispersal in West Indian terrestrial vertebrates. *Proc. Natl Acad. Sci. USA*, 89, 1909–1913.
1353 doi:10.1073/pnas.89.5.1909
1354

1355 Hine A.C., Locker S.D., Tedesco L.P., Mullins H.T., Hallock P., Belknap D.F., Gonzales J.L.,
1356 Neuman A.C. and Snyder S.W, 1992. Megabreccia shedding from modern, low-relief
1357 carbonate platforms, Nicaraguan Rise. *Geol. Soc. Amer. Bull.*, 104, 928-943.
1358

1359 Iturralde-Vinent M. A., 2006. Meso-Cenozoic Caribbean palaeogeography: implications for
1360 the historical biogeography of the region. *Int. Geol. Rev.*, 48, 791-827.
1361

1362 Iturralde-Vinent M.A. and MacPhee R.D.E., 1999 Palaeogeography of the Caribbean region:
1363 implications for Cenozoic biogeography. *Bull. Am. Mus. Nat. Hist*, 238, 1–95.
1364

1365 Jany I., 1989. Néotectonique au sud des Grandes Antilles: Collision (ride de Beata, presqu'île
1366 de Bahoruco): Subduction (fosse de Los Muertos), transtension (passage d'Anegada). PhD
1367 Thesis, University Pierre et Marie Curie, 300 p.
1368

1369 Jany I., Scanlon K. M. and Mauffret, A., 1990. Geological interpretation of combined
1370 Seabeam, Gloria and seismic data from Anegada Passage (Virgin Islands, north Caribbean).
1371 *Mar. Geophys. Res.* 12, 173-196. <https://doi.org/10.1007/BF02266712>
1372

1373 Jolly W.T., Lidiak E.G., Schellekens J.H. and Santos, H., 1998. Volcanism, tectonics, and
1374 stratigraphic correlations in Puerto Rico. *Geol. Soc. Am. Spec. Pap.*, 322, 1–34.

1375
1376 Land L.S., MacKenzi F.E. and Gould S.J., 1967. Pleistocene history of Bermuda. *Geol. Soc.*
1377 *Amer. Bull.*, 78, 993-1106.
1378
1379 Larue D.K. and Warner AJ. 1991. Sedimentary basins of the NE Caribbean Plate boundary
1380 zone and their petroleum potential. *J. Petr. Geol.*, 14. [https://doi.org/10.1111/j.1747-](https://doi.org/10.1111/j.1747-5457.1991.tb00312.x)
1381 [5457.1991.tb00312.x](https://doi.org/10.1111/j.1747-5457.1991.tb00312.x)
1382
1383 Laurencin M., Marcaillou B., Graindorge D., Klingelhoefer F., Lallemand S., Laigle M. and
1384 Lebrun J.-F., 2017. The polyphased tectonic evolution of the Anegada Passage in the northern
1385 Lesser Antilles subduction zone. *Tectonics*, 36, 945–961.
1386 <https://doi.org/10.1002/2017TC004511>
1387
1388 Laurencin M., Graindorge D., Klingelhoefer F., Marcaillou B. and Evain M., 2018.
1389 Influence of increasing convergence obliquity and shallow slab geometry onto tectonic
1390 deformation and seismogenic behavior along the Northern Lesser Antilles zone. *Earth Planet.*
1391 *Sci. Lett.*, 492, 59-72
1392
1393 Lebrun J.F. and Lallemand S., 2017. Unpublished GARANTI cruise report.
1394 <http://dx.doi.org/10.17600/17001200>
1395
1396 Legendre L., 2018. Cinématique des déformations fragiles dans la partie Nord de l’arc des
1397 Petites Antilles. PhD Thesis, Université des Antilles.
1398
1399 Legendre L., Philippon M., Münch P., Leticée J. L., Noury M., Maincent, G., Cornée J.-J.,
1400 2018. Trench bending initiation: Upper plate strain pattern and volcanism. Insights from the
1401 Lesser Antilles arc, St Barthelemy Island, French West Indies. *Tectonics*, 37, 2777–2797.
1402 <https://doi.org/10.1029/2017TC004921>
1403
1404 Mac Donald R., Hawkesworth C. J. and Heath E., 2000. The Lesser Antilles volcanic chain:
1405 A study in arc magmatism. *Earth Sci. Rev.*, 49, 1–76.
1406
1407 MacPhee R. D. E., 2005. 'First' appearances in the Cenozoic land-mammal record of the
1408 Greater Antilles: significance and comparison with South American and Antarctic records. *J.*
1409 *Biogeogr.*, 32, 551-564.
1410
1411 MacPhee R.D.E. and Iturralde-Vinent M.A., 1995. Origin of the Greater Antillean land
1412 mammal fauna, 1: New Tertiary fossils from Cuba and Puerto Rico. *Am. Mus. Novit.* 3141, 1-
1413 30.
1414
1415 Mann P., Taylor F.W., Lawrence Edwards R. and Ku T., 1995. Actively evolving microplate
1416 formation by oblique collision and sideways motion along strike-slip faults: An example from
1417 the northeastern Caribbean plate margin. *Tectonophysics*, 246, 1-69.
1418
1419 Mann P., Hippolyte J.C., Grindlay N.R. and Abrams L.J., 2005. Neotectonics of southern
1420 Puerto Rico and its offshore margin, in: Mann, P. (Ed.), Active tectonics and seismic hazards
1421 of Puerto Rico, the Virgin Inlands and off-shore areas. *Geol. Soc. Am. Spec. Paper*, 385, 115-
1422 138.
1423
1424 Marcaillou B. and Klingelhoefer F., 2013. ANTITHESIS-1-Leg1 Cruise, RV L'Atalante,
1425 doi:10.17600/13010070.

1426
1427 Marcaillou, B., Klingelhoefer, F., 2016. ANTITHESIS-3 Cruise, RV Pourquoi Pas?,
1428 doi:10.17600/16001700
1429
1430 Marivaux L., Vélez-Juarbe J., Merzeraud G., Pujos F., Viñola López L. W., Boivin M.,
1431 Santos-Mercado H., Cruz E. J., Grajales A., Padilla J., Vélez-Rosado K. I., Philippon M.,
1432 Léticée J.-L., Münch P. and Antoine P.-O., 2020. Early Oligocene chinchilloid caviomorphs
1433 from Puerto Rico and the initial rodent colonization of the West Indies. *Proc. Roy. Soc. B*,
1434 287, 20192806.
1435
1436 Martin-Kaye P.H.A., 1969. A summary of the geology of the Lesser Antilles. *Overseas Geol.*
1437 *Miner. Resour.*, 10, 172-206.
1438
1439 Mascle A. and Westercamp D., 1983. Géologie d'Antigua, Petites Antilles. *Bull. Soc. Géol.*
1440 *Fr.*, 7, 855-866.
1441
1442 Matchette-Downes C., 2007. Saba Bank, Dutch Antilles petroleum potential.Saba Bank
1443 Petroleum Ressources, 19 pp. <https://www.mdoil.co.uk/pdfs/Curacao.pdf>
1444
1445 Mauffret A. and Jany I., 1990. Collision et tectonique d'expulsion le long de la frontière Nord-
1446 Caraïbe. *Oceanologica Acta*, spec. vol. 10, 97-116.
1447
1448 McCann W.R. and Sykes L.R., 1984. Subduction of aseismic ridges beneath the Caribbean
1449 Plate: Implications for the tectonics and seismic potential of the northeastern Caribbean. *J.*
1450 *Geophys.Res.* 89, 4493-4519, [doi:10.1029/JB089iB06p04493](https://doi.org/10.1029/JB089iB06p04493).
1451
1452 Mittermeier R. A., Turner W. R., Larse, F. W., Brooks T. M. and Gascon, C., 2011.Global
1453 Biodiversity Conservation: The Critical Role of
1454 Hotspots in Biodiversity Hotspots. Springer (eds Zachos F. E. and Habel J. C.), 3–22.
1455
1456 Montaggioni L. and Braithwaite C.J.R., 2009. Structure, zonation and dynamic patterns of
1457 coral reef communities. *Developments in Marine Geology*, 5, 67-122, Elsevier. [doi:](https://doi.org/10.1016/S1572-5480(09)05003-9)
1458 [10.1016/S1572-5480\(09\)05003-9](https://doi.org/10.1016/S1572-5480(09)05003-9)
1459
1460 Multer H.G., Weiss M.P. and Nicholson D.V., 1986. Antigua; reefs, rocks and highroads of
1461 history. Leeward Island Science Associates, St John's, Antigua, Contrib. 1, 116 pp.
1462
1463 Münch P., Lebrun J.-F, Cornée J.-J., Thinon I., Guennoc P., Marcaillou B., Randrianasolo A.
1464 and the KASHALLOW TEAM, 2013. Pliocene to Pleistocene carbonate systems of the
1465 Guadeloupe archipelago, French Lesser Antilles: a land and sea study. *Bulletin de la Société*
1466 *géologique de France*, 184, 99-110.
1467
1468 Münch, P., Cornée, J.-J., Lebrun, J.F., Quillévéré, F., Vérati, C., Melinte-Dobrinescu, M.,
1469 Demory, F.,Smith, M.J., Jourdan, X., Lardeaux, J.-M., De Min L., Léticée J.-L. and
1470 Randrianasolo A., 2014. Pliocene to Pleistocene vertical movements in the forearc of the
1471 Lesser Antilles subduction: insights from chronostratigraphy of shallow-water carbonate
1472 platforms (Guadeloupe archipelago). *J. Geol. Soc. London*, 171, 329-341.
1473
1474 Myers N., Russell A., Mittermeier R.A., Mittermeier C.G., da Fonseca G.A.B. and Kent J.,
1475 2000. Biodiversity hotspots for conservation priorities. *Nature*, 403, 853-858.
1476

- 1477 Nagle F., Stipp J. J. and Fisher D. E., 1976. K-Ar geochronology of the limestone caribbees
1478 and Martinique, Lesser Antilles, West Indies. *Earth Planet. Sci. Lett.*, 29, 401–412.
1479
- 1480 Nairn A. and Stehli F.G. eds., 1975. Geology of the Caribbean crust, Gulf of Mexico and the
1481 Caribbean. Plenum press, 1975.
1482
- 1483 Neill I., Kerr A. C., Hastie A. R., Stanek K. P. and Millar I. L., 2011. Origin of the Aves Ridge
1484 and Dutch–Venezuelan Antilles: Interaction of the Cretaceous ‘Great Arc’ and Caribbean–
1485 Colombian Oceanic Plateau? *J. Geol. Soc. London*, 168, 333–348.
- 1486 Padron C., Klingelhoefer F. Marcaillou B., Lebrun J.-F., Lallemand S., Garrocq C., Laigle
1487 M., Roest W. R., Schenini L., Beslier M.-O., Graindorge D., Gay A., Audemard F., Münch Ph.
1488 and the GARANTI Cruise Team, 2020. Deep Structure of the Grenada Basin From Wide-
1489 Angle Seismic, Bathymetric and Gravity Data. *J. Geoph. Res.*, 126, e2020JB020472.
1490 <https://doi.org/10.1029/2020JB020466>
- 1491 Philippon M. and Corti G., 2016. Obliquity along plate boundaries. *Tectonophysics*, 693, 171-
1492 182. <https://doi.org/10.1016/j.tecto.2016.05.033>
1493
- 1494 Philippon M., Cornée J.-J., Münch P., van Hinsbergen D.J.J., BouDagher-Fadel M., Gailler
1495 L., Quillévéré F., Boschman L., Montheil L., Gay A., Lebrun J.-F., Lallemand S., Marivaux
1496 L. and Antoine P.O., 2020a. Eocene intra-plate shortening responsible for the rise of a fauna
1497 pathway in the northeastern Caribbean realm. *Plos-ONE*, 15(10): e0241000.
1498 <https://doi.org/10.1371/journal.pone.0241000>
1499
- 1500 Philippon M., Boschman L.M., Gossink L.A.W., Munch P., Cornée J.-J., Boudagher-Fadel
1501 M., Lécécée J.L., Lebrun J.-F. and Van Hinsbergen D.J.J., 2020b. Paleomagnetic evidence
1502 from St. Barthélemy Island for post-Eocene rotation and deformation in the forearc of the
1503 curved Lesser Antilles subduction zone. *Tectonophysics*, 777, 228323.
1504 <https://doi.org/10.1016/j.tecto.2020.228323>
1505
- 1506 Pindell J. L. and Kennan L., 2009. Tectonic evolution of the Gulf of Mexico, Caribbean and
1507 northern South America in the mantle reference frame: an update. Geological Society, London,
1508 Special Publications 328, 1-55, [doi:10.1144/SP328.1](https://doi.org/10.1144/SP328.1).
1509
- 1510 Presslee S., Slater, G. J., Pujos F., Forasiepi A. M., Fischer R., Molloy K., Mackie M., Olsen J.
1511 V., Kramarz A. G., Taglioretti M., Scaglia F., Lezcano M., Lanata J. L., Southon J., Feranec
1512 R., Bloch J. I., Hajduk A., Martin F. M., Salas-Gismondi R., Reguero M. A., de Muizon C.,
1513 Greenwood A., Chait B. T., Penkman K., Collins M. and MacPhee R. D. E., 2019.
1514 Palaeoproteomics resolves sloth relationships. *Nat. Ecol. Evol.*, 3, 1121–1130.
1515
- 1516 Railsback L.B., Gibbard P.L., Head M.J., Voarintsoa N.R.G. and Toucanne S., 2015. An
1517 optimized scheme of lettered marine isotope substages for the last 1.0 million years, and the
1518 climatostratigraphic nature of isotope stages and substages. *Quat. Sci. Rev.*, 111, 94–106.
1519 Rankin D.W., 2002. Geology of St John, U.S. Virgin Islands. U.S. Geol. Surv. Prof. Paper
1520 1631, 36 pp.
1521
- 1522 Reed F.R.C., 1921. The Geology of the British Empire. Edward Arnold, London.
1523 Robinson E. D., Paytan A. D. and Chien C. T., 2017. Strontium isotope dates for the
1524 Oligocene Antigua Formation, Antigua, WI. *Caribb. J. Earth Sci.*, 50, 11-18.
1525

- 1526 Roca A. L., Bar-Gal G., Eizirik E., Helgen K. M., Maria R., Springer M. S., O'Brien, S. J. and
 1527 Murphy W. J., 2004. Mesozoic origin for West Indian insectivores. *Nature*, 429, 649-651.
 1528
- 1529 Roksandic M.M., 1978. Seismic facies analysis concepts. *Geophys. Prospect.*, 26, 383-398.
 1530 Russell R. J. and McIntire W. J. 1966. Barbuda reconnaissance. *Tech. Rep. coastal Stud. Inst*
 1531 *La St Univ.*, 11 (J), 1-53.
 1532
- 1533 Samper A, Quidelleur X, Lahitte P, Mollex D. 2007. Timing of effusive volcanism and
 1534 collapse events within an oceanic arc island: Basse-Terre, Guadeloupe archipelago (Lesser
 1535 Antilles Arc). *Earth Planet. Sci. Letters* 258, 175–191. [DOI: 10.1016/j.epsl.2007.03.030](https://doi.org/10.1016/j.epsl.2007.03.030).
- 1536 Scotese, C.R., 2016. PALEOMAP PaleoAtlas for GPlates and the PaleoData Plotter Program,
 1537 PALEOMAP Project, <http://www.earthbyte.org/paleomap---paleoatlas---for---gplates>
 1538
- 1539 Speed R. C., Gerhard L. C. and McKee E. H., 1979. Ages of deposition, deformation, and
 1540 intrusion of Cretaceous rocks, eastern St Croix, Virgin Islands. *Geol. Soc. Amer. Bull.*, 90, 629-
 1541 632.
 1542
- 1543 Stéphan J.F., Mercier de Lépinay B., et al., 1990. Paleogeodynamics maps of the Caribbean-14
 1544 steps from Lias to Present. *Bull. Soc. géol. Fr.* 6, 915-919.
 1545
- 1546 Tucker M.E. and Wright, V.P., 1990. Diagenetic processes, products and environments. *In:*
 1547 *Carbonate Sedimentology*. Blackwell Publishing Ltd, Oxford, U.K., 314–364.
 1548
- 1549 Vail P. R., Mitchum R. M. and Thompson S., 1977, Seismic stratigraphy and global changes of
 1550 sea level, Part 3: Relative changes of sea level from coastal onlap. *In:* *Seismic Stratigraphy—*
 1551 *Applications to Hydrocarbon Exploration* (Ed. Payton, C. W.): American Association
 1552 *Geologists Memoir*, 26, 83-97.
 1553
- 1554 Van Duyle F.C. and Meesters E.H., 2018. Cruise report RV Pelagia 64PE433, Saba, St Eustatius
 1555 and Saba Bank. 26 February-10 March 2018, St Maarten-St Maarten (NICO expedition leg 6).
 1556 [https://www.dcbd.nl/document/cruise-report-rv-pelagia-64pe433-saba-st-eustatius-and-saba-bank-](https://www.dcbd.nl/document/cruise-report-rv-pelagia-64pe433-saba-st-eustatius-and-saba-bank-benthic-habitat-mapping)
 1557 [benthic-habitat-mapping](https://www.saba-news.com/saba-bank-has-the-deepest-and-largest-marine-sinkholes-in-the-world/) and [https://www.saba-news.com/saba-bank-has-the-deepest-and-largest-](https://www.saba-news.com/saba-bank-has-the-deepest-and-largest-marine-sinkholes-in-the-world/)
 1558 [marine-sinkholes-in-the-world/](https://www.saba-news.com/saba-bank-has-the-deepest-and-largest-marine-sinkholes-in-the-world/)
 1559
- 1560 Van Wagoner C., Posamentier H. W., M. Mitchum R., Vail P. R., Sarg J. F., Loutit T. S. and J.
 1561 Hardenbol J., 1988. An overview of the fundamentals of sequence stratigraphy and key
 1562 definitions. *In:* *Sea-Level Changes—An Integrated Approach*, SEPM Special Publication, 42,
 1563 39-45
 1564
- 1565 Wade B.S., Pearson P.N., Berggren W.A. and Paëlike H., 2011. Review and revision of
 1566 Cenozoic tropical planktonic foraminiferal biostratigraphy and calibration to the geomagnetic
 1567 polarity and astronomical time scale. *Earth Sci. Rev.*, 104, 111-142.
 1568
- 1569 Warner A.J., 1990. The Cretaceous age sediments of the Saba Bank and their petroleum
 1570 potential. *In:* Larue DK, Draper G (eds), *Trans. 12 th Caribbean Conference, St Croix. Miami*
 1571 *Geol. Soc.*, South Miami, 341–354
 1572
- 1573 Watters D., Donahue J. and Stuckenrath R., 1991. Paleoshorelines and the prehistory of
 1574 Barbuda, West Indies. *In:* *Paleoshorelines and Prehistory: an investigation method* (Jonhson
 1575 L.L. ed.). CRC Press, London, 15-51.

1576
1577 Weiss M.P., 1994. Oligocene limestones of Antigua, West Indies: Neptune succeeds
1578 Vulcan. *Caribb. J. Earth Sci.*, 30, 1-29.
1579
1580 Westercamp D., 1988. Magma generation in the Lesser Antilles: geological constraints.
1581 *Tectonophysics*, 149, 145-163. [doi: 10.1016/0040-1951\(88\)90123-0](https://doi.org/10.1016/0040-1951(88)90123-0)
1582
1583 Westercamp D., Andréieff P., Bouysse P. and Mascle A.,1985. The Grenadines, southern
1584 Lesser Antilles. Part I. Stratigraphy and volcano-structural evolution. *Carr. Geod.*
1585
1586 Woods C. A., Borroto Paéz R. and Kilpatrick C. W. 2001. Insular patterns and radiations of
1587 West Indian rodents. *In: Biogeography of the West Indies: Patterns and Perspectives* (Woods
1588 C. A. and Sergile F. E. Eds), 335-353. Boca Raton: CRC Press.
1589
1590 Wright V. P. and Burchette T. P., 1996. Shallow-water carbonate environments. *In:*
1591 *Sedimentary Environments: Processes, Facies, and Stratigraphy* (ed. H. G. Reading), 325–94.
1592 Oxford, Blackwell Science.
1593
1594 Zachariasse W.J., van Hinsbergen D.J.J. and Fortuin A.R., 1988. Mass wasting and uplift on
1595 Crete and Karpathos during the early Pliocene related to initiation of south Aegean left-
1596 lateral, strike-slip tectonics. *Geol. Soc. Amer. Bull.*, 120, 976–993. [doi: 10.1130/B26175.1](https://doi.org/10.1130/B26175.1)